Arrays of cryogenic microcalorimeters for high precision x-ray and gamma-ray measurements

Joel Ullom

Chief, Quantum Sensors Division, NIST

Lecturer, Department of Physics, University of Colorado

joel.ullom@nist.gov

June 20, 2025

- NIST = National Institute of Standards and Technology, branches in Boulder Colorado and Gaithersburg Maryland.
- US National Metrology Institute, part of Department of Commerce. Similar to NPL or PTB.

Outline

1. Introduction to microcalorimeter arrays
2. Examples of applications
3. Current work to improve the technology

Many contributors from NIST, the University of Colorado Boulder, Los Alamos, Pacific Northwest National Lab, Idaho National Lab, the HEATES and PAX collaborations, Stanford, SLAC, BESSYII, Brookhaven National Lab, and elsewhere …

Superconducting microcalorimeters

thin-film sensor

300 um

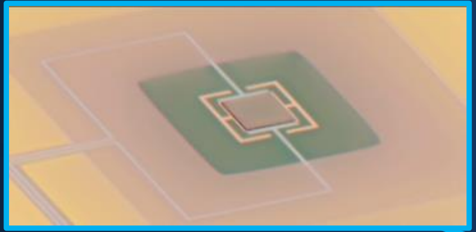

pixelated array of sensors

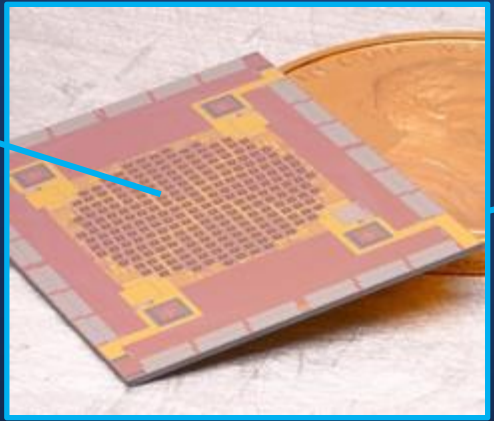

packaged array and superconducting readout circuitry

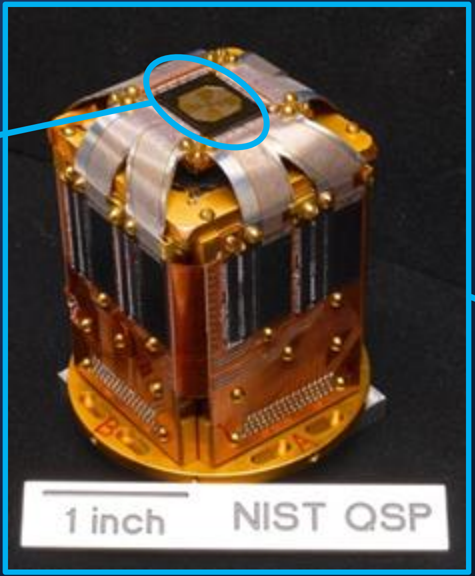

a complete instrument including a 50 mK refrigerator

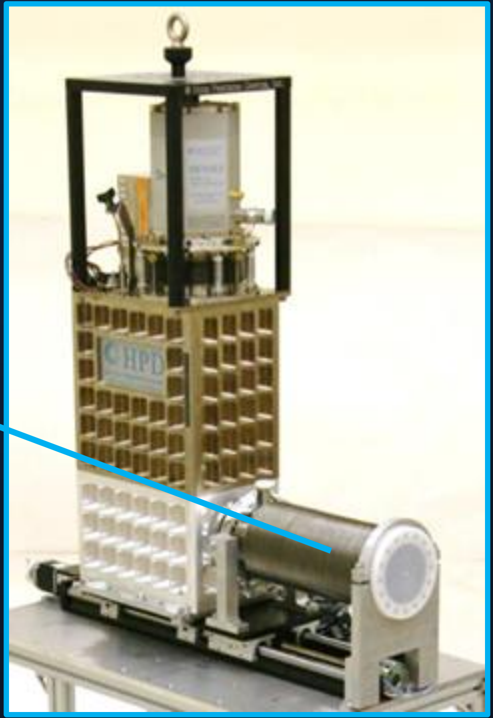

1 m

Superconducting microcalorimeters

thin-film sensor

300 um

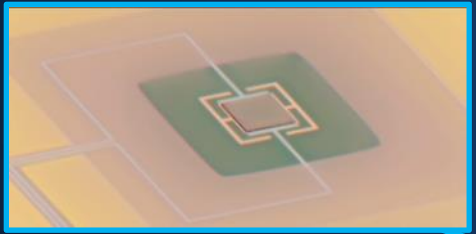

pixelated array of sensors

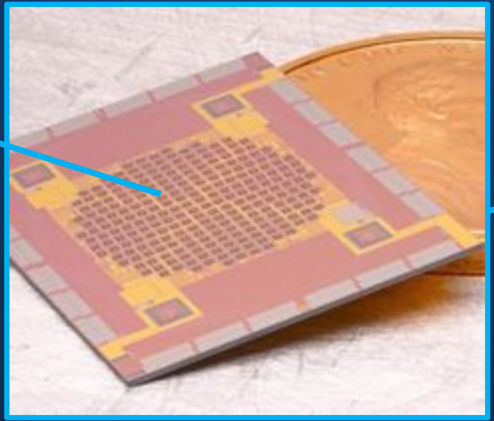

packaged array and superconducting readout circuitry

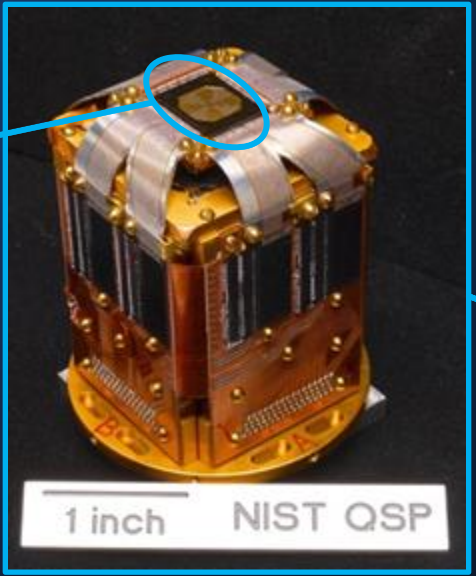

a complete instrument including a 50 mK refrigerator

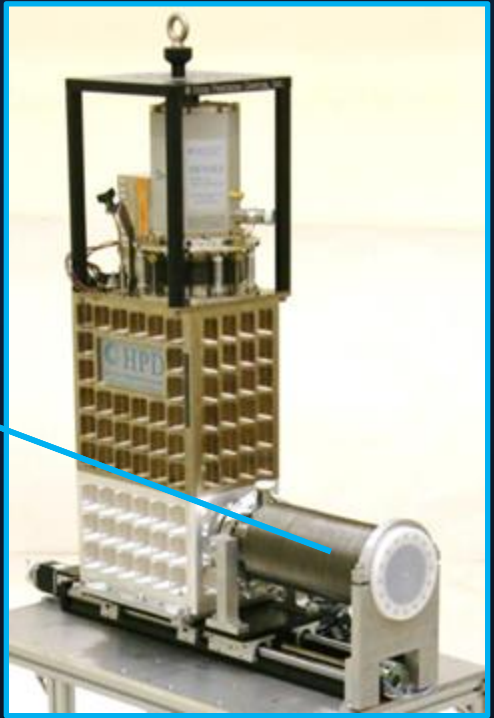

1 m

10 keV sensor: ~0.1 mm^2, 1000 sensors = 100 mm^2 located 30 mm from source

100 keV sensor: ~1 mm^2, 1000 sensors = 1000 mm^2 located 30 mm from source

What is a microcalorimeter?

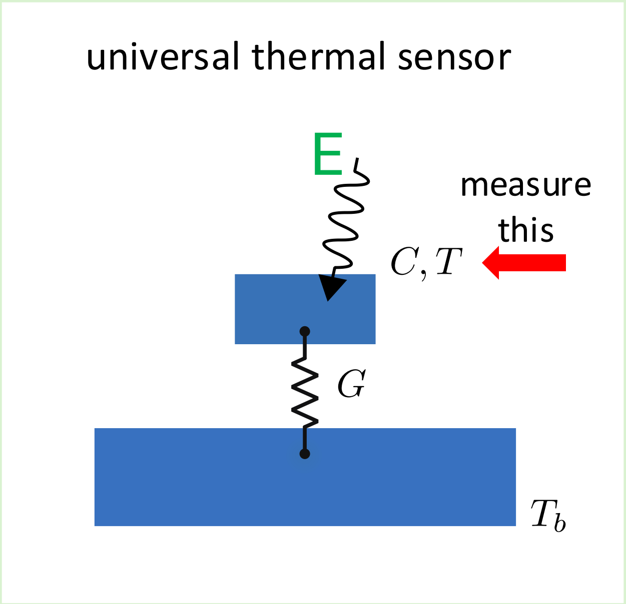

microcalorimeter: a device that measures deposited energy via a temperature change

Why millikelvin temperatures?

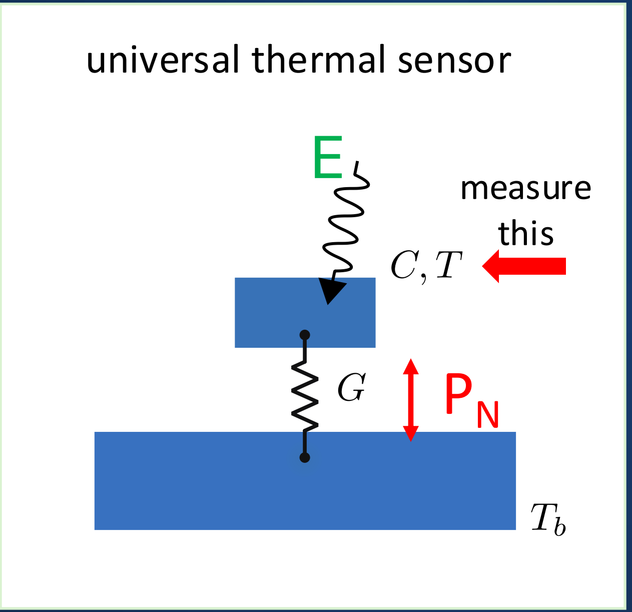

- Temperatures near 0.1 K suppress noise, enabling precise energy and power measurements

$$\Delta E = (2\ k_b\ T^2\ C(T))^{1/2}\ \ J$$

Why millikelvin temperatures?

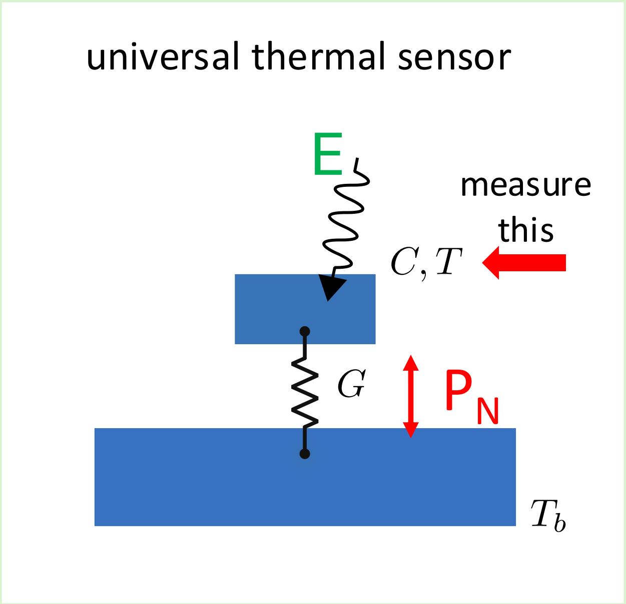

consider a 6 keV x-ray: E = 1 fJ

consider a sensor consisting of a 250 x 250 x 0.25 μm^3 film of gold at 0.1 K ➡ C = 0.1 pJ/K ➡ ΔE = 1.0 eV

how does this compare to other x-ray detectors?
for silicon sensor, ΔE = 125 eV

- Temperatures near 0.1 K suppress noise, enabling precise energy and power measurements

$$\Delta E = (2\, k_b\, T^2\, C(T))^{1/2} \ \ \mathrm{J}$$

Transition-Edge Sensor (TES) thermometer

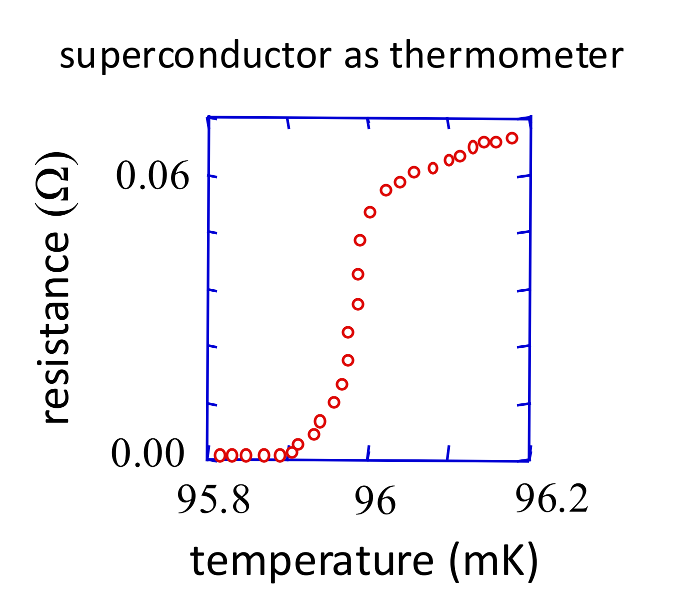

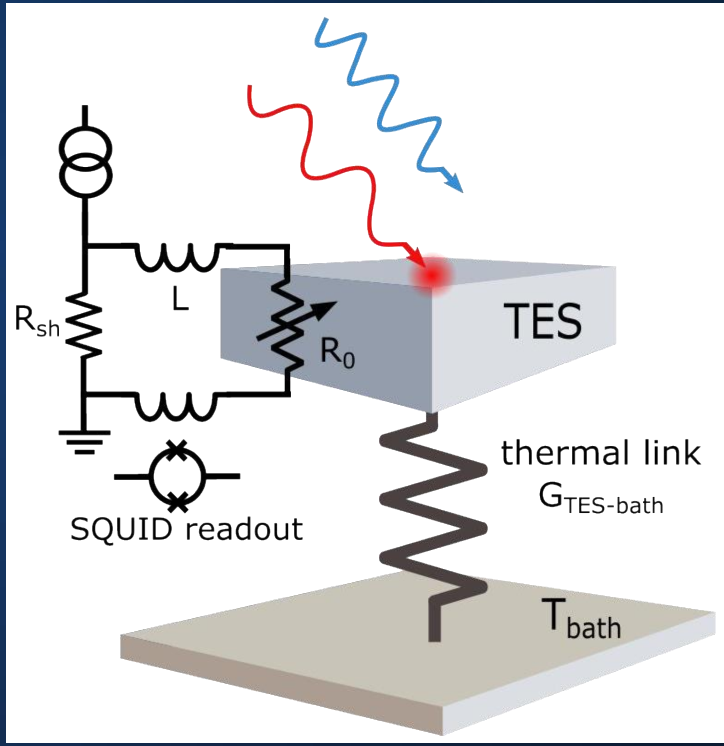

- TES = a thin-film structure
- TES is voltage-biased using a current source and a parallel shunting resistor R_{sh}
- The TES is placed in series with a SQUID ammeter that measures its current

SQUID = Superconducting Quantum Interference Device, a thin-film circuit that transduces current or magnetic flux to voltage

TES response to deposited energy

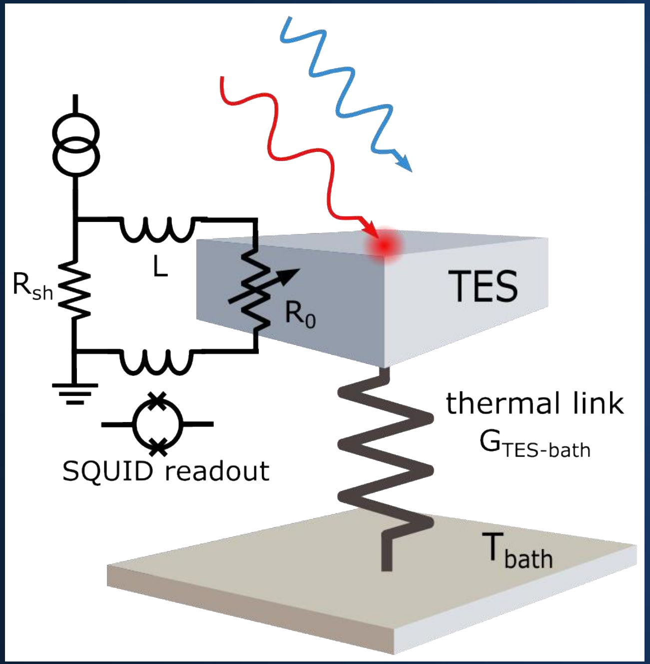

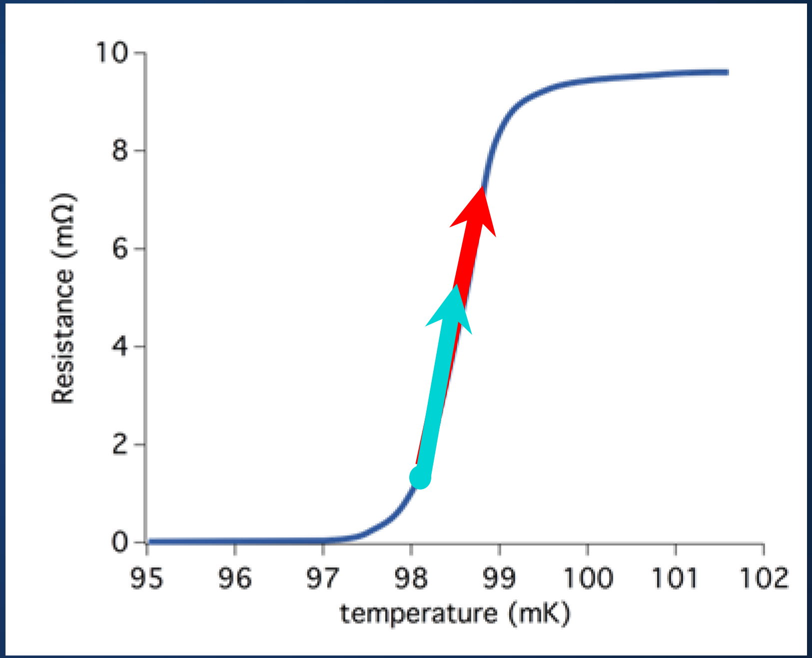

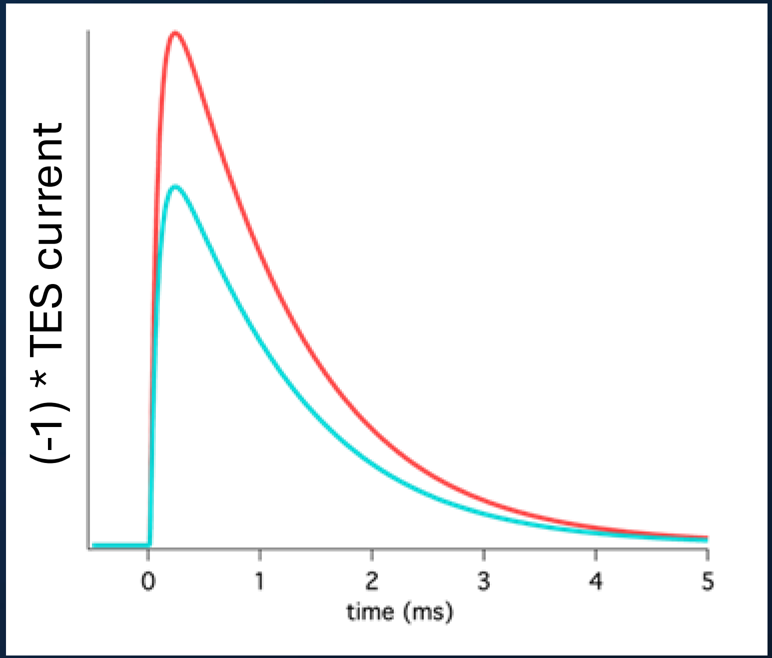

- deposited energy causes TES temperature and resistance to increase
- a resistance increase under voltage bias causes current and power to decrease (Irwin, APL 1995)
- then, the TES cools back to its quiescent state
- the height (and area) of the current pulse reveal the deposited energy

Multiplexed TES readout

- electrical connections between 300 K and 100 mK are mechanically complex and produce a thermal load
- in an array with 100s or 1000s of sensors, it is impractical to have a dedicated amplifier chain for each sensor
- instead, sensors are multiplexed: sensor signals are encoded with an orthogonal basis set, combined, amplified, passed to 300 K, and then demodulated
- there are several possible multiplexing schemes:

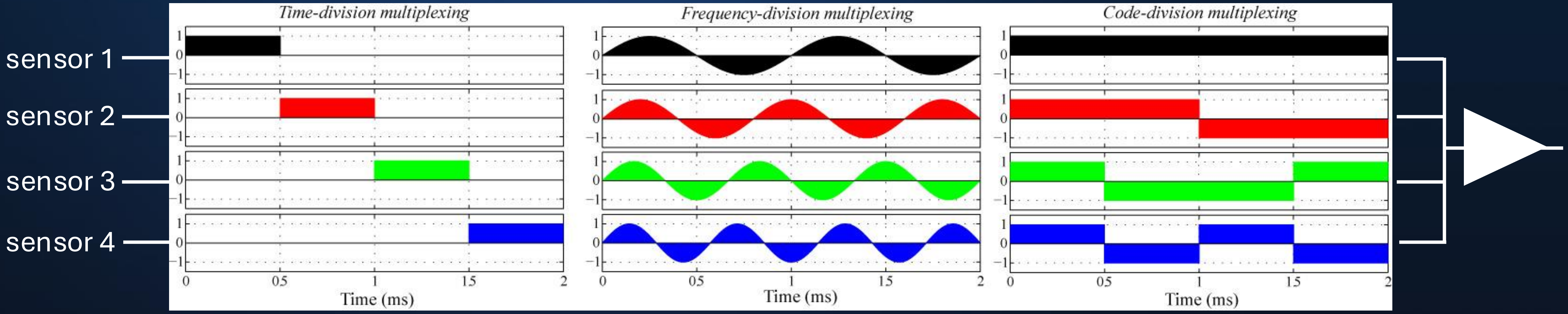

Frequency-division multiplexing at GHz frequencies = state-of-the-art

Microwave SQUID multiplexing

- Frequency-specific microresonators coupled to a common feedline and amplifier
- An RF-SQUID embedded in each resonator. Each TES sensor coupled to an RF-SQUID
- Several GHz of bandwidth per amplifier channel, 100s to 1000s of sensors per amplifier

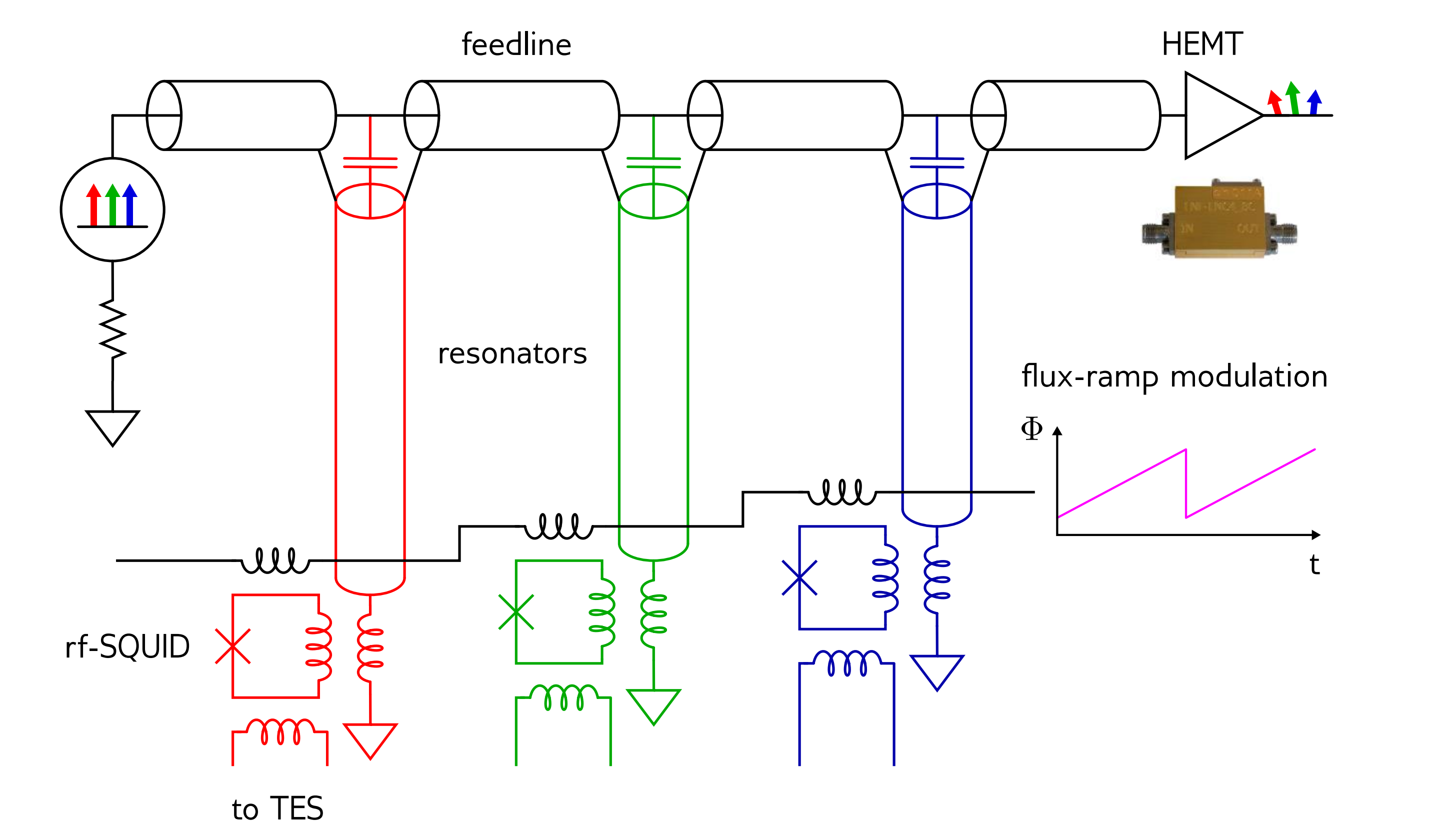

- microwave resonators terminated in variable inductor (RF-SQUID), which is coupled to TES detector
- change in detector resistance
  → change in current
  → change in termination inductance
  → change in resonant frequency
  → change in transmitted amplitude and phase
- sensor signals encoded as phase shift in response to linearizing flux ramp

Irwin and Lehnert, Applied Physics Letters 85, 2107 (2004)

Actual multiplexer

- Tens of microwave resonators coupled to common feedline
- Frequencies between 4 and 8 GHz
- Resonator widths between 100 kHz and ~10 MHz

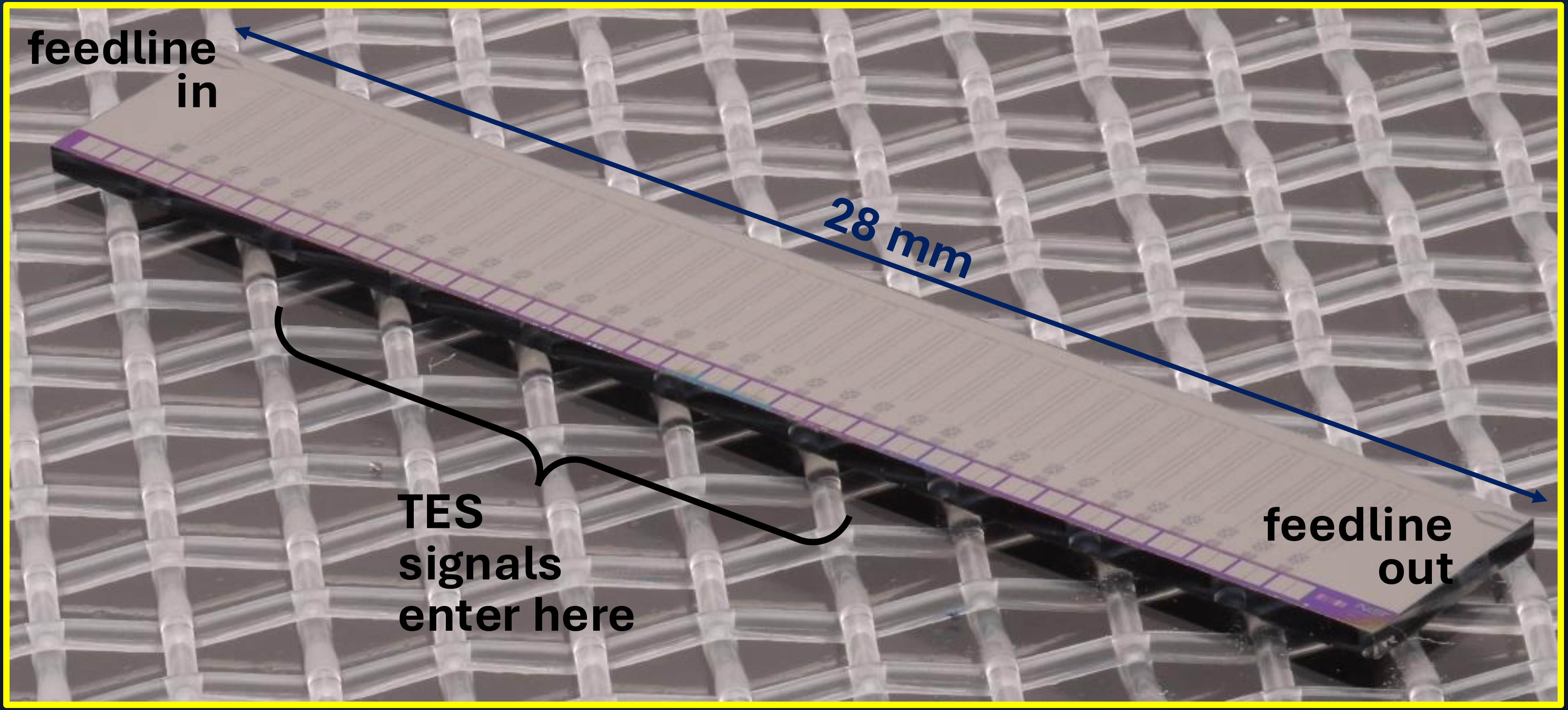

Modern cryogenics: no liquid cryogens

commercial adiabatic demagnetization refrigerator (NIST-designed)

1 m

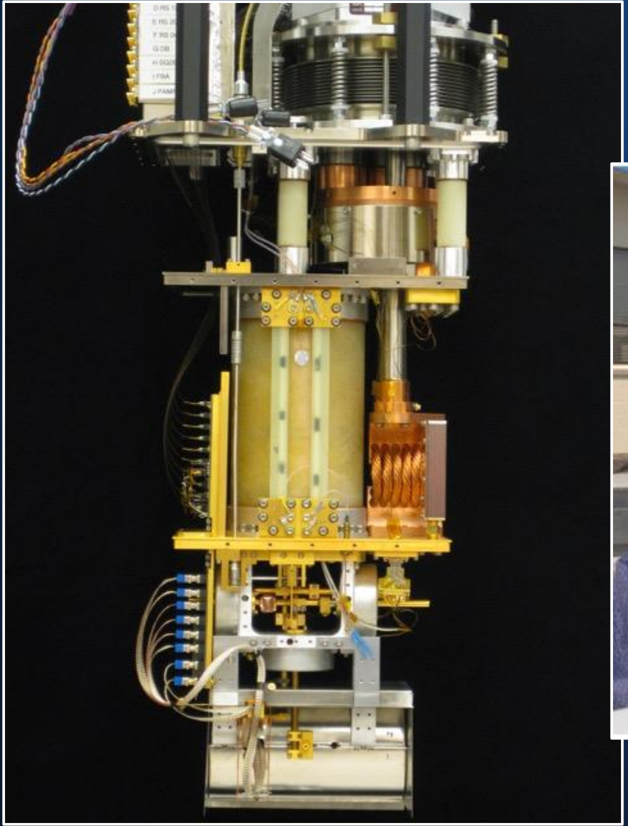

modest cooling power but easily brought to photon sources

commercial dilution refrigerator (right) on custom stand to mate with electron microscope (left)

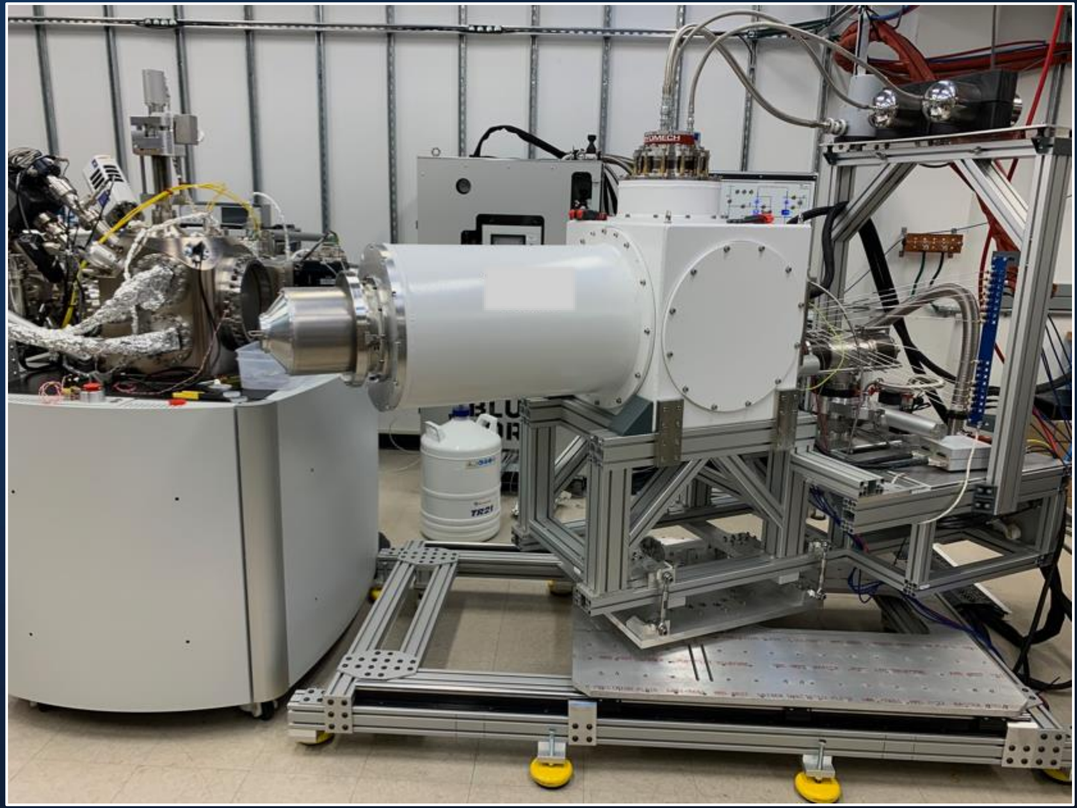

DR has abundant cooling power for large sensor arrays

Why microcalorimeter arrays?

- high photon collection efficiency combined with excellent resolving power
- energy-dispersive, so response is broadband and resolving power is unchanged by extended sources

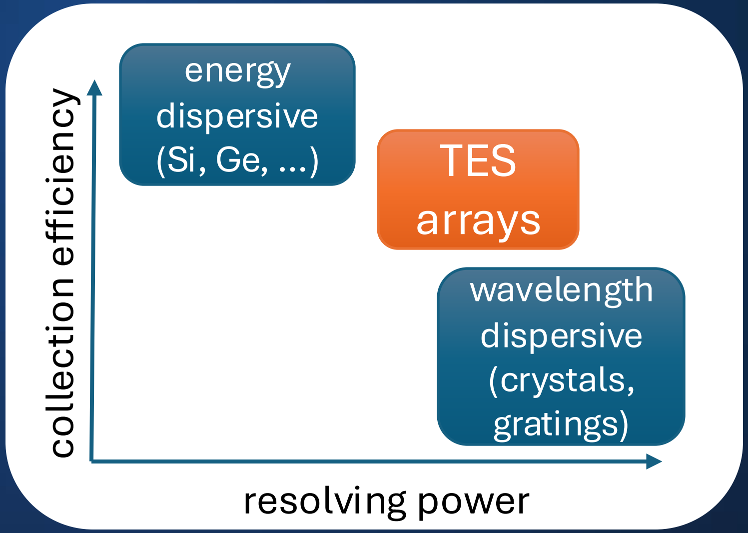

	1,000 TESs, 100keV	Xtal, 100 keV
resolving power ($E/\Delta E$)	$2\text{-}4\times10^3$	1.3×10^3
collecting efficiency ($\eta d\Omega/4\pi$)	10^{-2}	8×10^{-8}

comparable

10^5 x

Efficiency advantage present at other energies too; will discuss soft x-rays later

See Paul, PRL 2021 and Beyer J Phys B 2015

Absolute energy calibration

- Some experiments require an absolute energy measurement
- Microcalorimeters are nonlinear so calibration is an important task

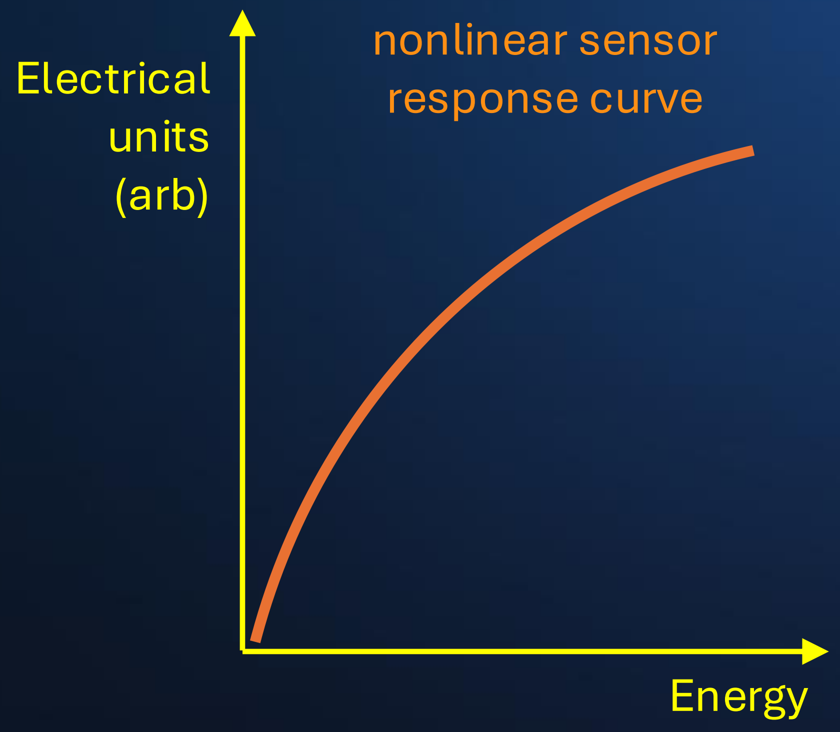

For TESs

$I(t) = V_b/(R_o + \Delta R(t))$ where $R \equiv R(I,T)$, a surface whose shape does not have a simple form known from theory

Absolute energy calibration

- Some experiments require an absolute energy measurement
- Microcalorimeters are nonlinear so calibration is an important task
- Calibrating microcalorimeters requires narrow spectral features at known energies

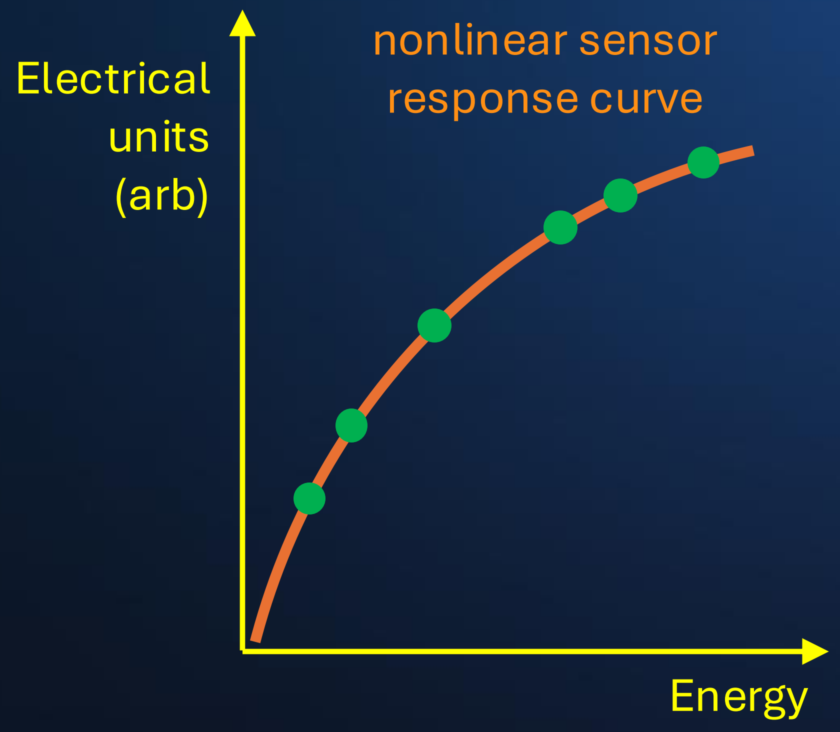

For TESs

$I(t) = V_b/(R_o + \Delta R(t))$ where $R \equiv R(I,T)$, a surface whose shape does not have a simple form known from theory

Use cubic smoothing spline or polynomial to describe curve

Application examples

- determination of atomic fundamental parameters
- spectroscopy of exotic atoms (Tadashi just covered this)
- analysis of nuclear materials
- x-ray astrophysics (mentioned earlier this week)
- photonic quantum computing
- synchrotron science
- …

Application examples

- determination of atomic fundamental parameters
- spectroscopy of exotic atoms   (Tadashi just covered this)
- analysis of nuclear materials
- x-ray astrophysics (mentioned earlier this week)
- photonic quantum computing
- synchrotron science
- …

X-ray science relies on atomic fundamental parameters

NIST standard reference database SRD-128 of x-ray energies

Also Deslattes et al., *Rev. Modern Phys.* **72**, 33-99 (2003)

Deslattes *et al.*: X-ray transition energies 65

TABLE V. (*Continued*).

Designation	Theory Energy (eV)	Experiment Energy (eV)	Experiment Blend	Ref.	Designation	Theory Energy (eV)	Experiment Energy (eV)	Experiment Blend	Ref.
KN_3 ($K\beta_2^{I}$)	41774.3(14)	41774.4(42)	$KN_{2,3}$	1	KN_2 ($K\beta_2^{II}$)	43322.(16)#	43335.(22)	$KN_{2,3}$	1
KN_4 ($K\beta_4^{II}$)	41872.4(45)				KN_3 ($K\beta_2^{I}$)	43344.9(14)	43335.(22)	$KN_{2,3}$	1
KN_5 ($K\beta_4^{I}$)	41876.35(97)				KN_4 ($K\beta_4^{II}$)	43449.2(42)#			
K edge	41994.11(75)	42002.(11)		1	KN_5 ($K\beta_4^{I}$)	43452.3(10)			
L_1M_1	5326.9(17)				K edge	43575.27(79)	43574.(11)		1
L_1M_2 ($L\beta_4$)	5497.2(22)	5498.1(14)		1	K edge (c)		43571.90(60)		
L_1M_3 ($L\beta_3$)	5593.5(21)	5591.8(11)		1	L_1M_1	5548.7(18)			
L_1M_4 ($L\beta_{10}$)	5881.9(19)	5884.0(17)		1	L_1M_2 ($L\beta_4$)	5723.4(22)	5721.6(12)		1
L_1M_5 ($L\beta_9$)	5903.2(18)	5902.8(17)		1	L_1M_3 ($L\beta_3$)	5828.5(21)	5827.801(52)		3
L_1N_1	6530.7(46)				L_1M_4 ($L\beta_{10}$)	6123.9(19)	6124.97(41)		1,29,30
L_1N_2 ($L\gamma_2$)	6597.(16)	6598.0(21)		1	L_1M_5 ($L\beta_9$)	6147.7(18)	6148.82(41)		1,29,30
L_1N_3 ($L\gamma_3$)	6617.0(17)	6615.9(21)		1	L_1N_1	6809.4(46)			
L_1N_4	6715.1(48)				L_1N_2 ($L\gamma_2$)	6877.(16)#	6884.03(34)		1,29,30
L_1N_5	6719.0(13)				L_1N_3 ($L\gamma_3$)	6899.8(17)	6900.44(34)		1,29,30
L_1N_6	6824.3(15)				L_1N_4	7004.1(45)#	7007.74(36)	$L_1N_{4,5}$	29,30
L_1 edge	6836.8(11)	6834.4(28)		1	L_1N_5	7007.2(13)	7007.74(36)	$L_1N_{4,5}$	29,30
L_1 edge (c)		6832.0(12)			L_1N_6	7117.2(15)	7122.1(20)	$L_1N_{6,7}$	30
L_2M_1 ($L\eta$)	4933.7(12)	4935.6(87)		1	L_1 edge	7130.2(11)	7129.52(61)		1
L_2M_2	5104.0(15)				L_1 edge (c)		7129.47(72)		
L_2M_3 ($L\beta_{17}$)	5200.4(14)				L_2M_1 ($L\eta$)	5145.6(12)	5145.25(17)		3
L_2M_4 ($L\beta_1$)	5488.7(12)	5488.9(11)		1	L_2M_2	5320.3(15)			
L_2M_5	5510.0(11)				L_2M_3 ($L\beta_{17}$)	5425.4(14)	5424.4(12)		30
L_2N_1 ($L\gamma_5$)	6137.5(40)	6136.2(18)		1	L_2M_4 ($L\beta_1$)	5720.8(12)	5721.446(50)		3
L_2N_2	6204.(15)				L_2M_5	5744.6(11)			
L_2N_3	6223.8(10)				L_2N_1 ($L\gamma_5$)	6406.3(39)	6405.29(33)		1,30

$_{59}$Pr $_{60}$Nd

- 77% of L lines cite only publications at least 50 years old.
- Based largely on Bearden, *Rev. Modern Phys.* **39**, 78 (1967). This is [1] in SRD-128.
  - …and many of these data are from before 1950.
  - Yttrium Kα is a weighted mean of data from 1925, 1926, and 1928.
- Systematic errors, if ever understood, are long ago lost.
- X-ray-optical interferometry (XROI) tied x-ray λ to the SI meter only in the early 1970s.
- Stated uncertainty often > 0.3 eV.
- No M lines
- No width or shape information

Neodymium

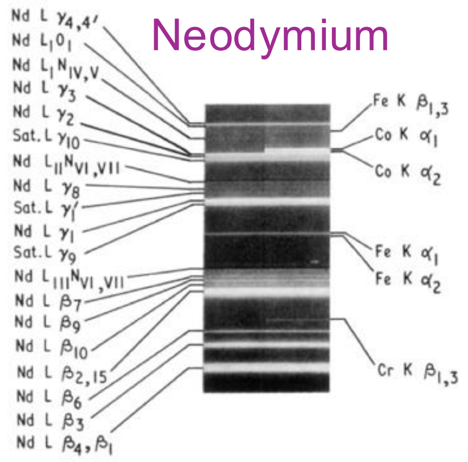

Figure 1. Part of the L emission spectrum of neodymium 60 (enlarged $\frac{4}{3}$ times) photographed with (100) planes of mica in the first order and showing the weak lines L_IO_I, $L_IN_{IV,V}$, $L_{II}N_{VI,VII}$ and $L_{III}N_{VI,VII}$.

From Gokhale & Shula, *J Phys. B* **3,** 438 (1970).

Modernizing lanthanide L lines

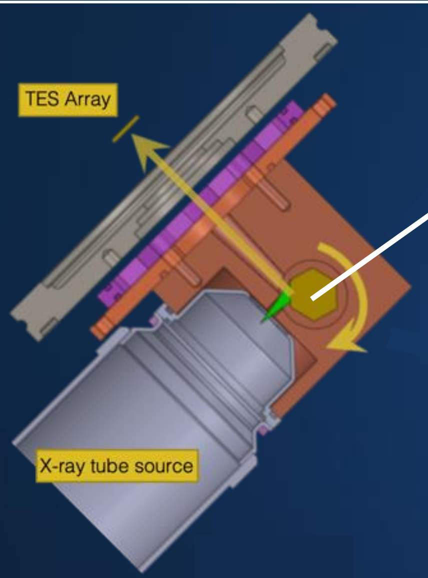

rotating 6-sided sample holder

calibration spectra

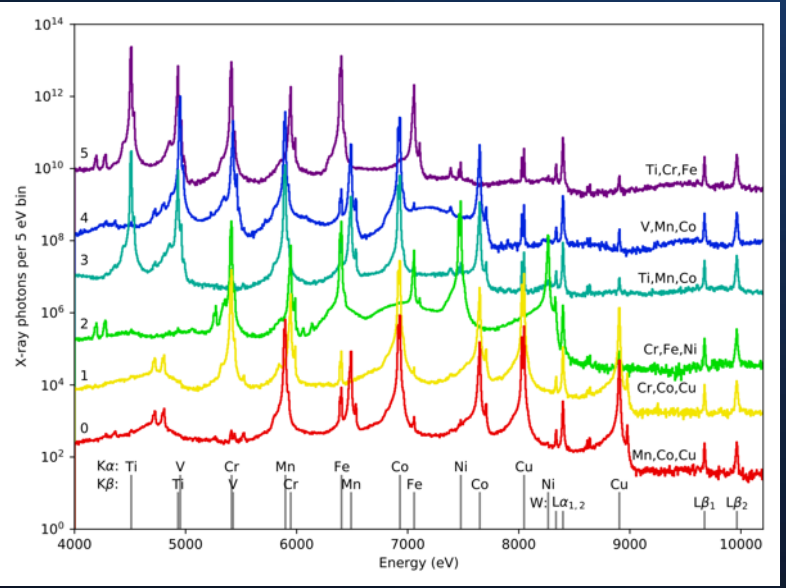

TES spectra of Ho, Tb, Nd, and Pr

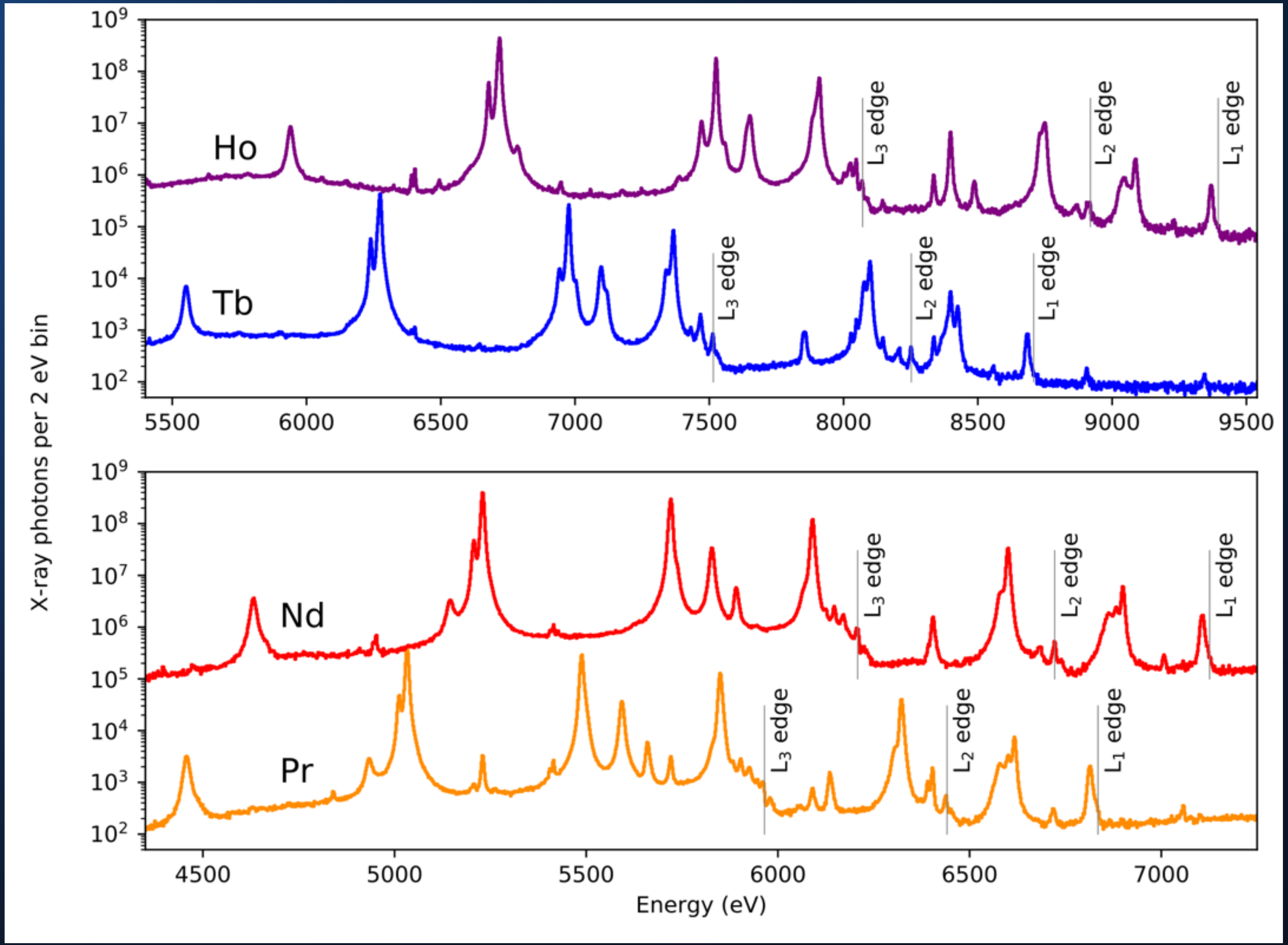

Close-up of TES data

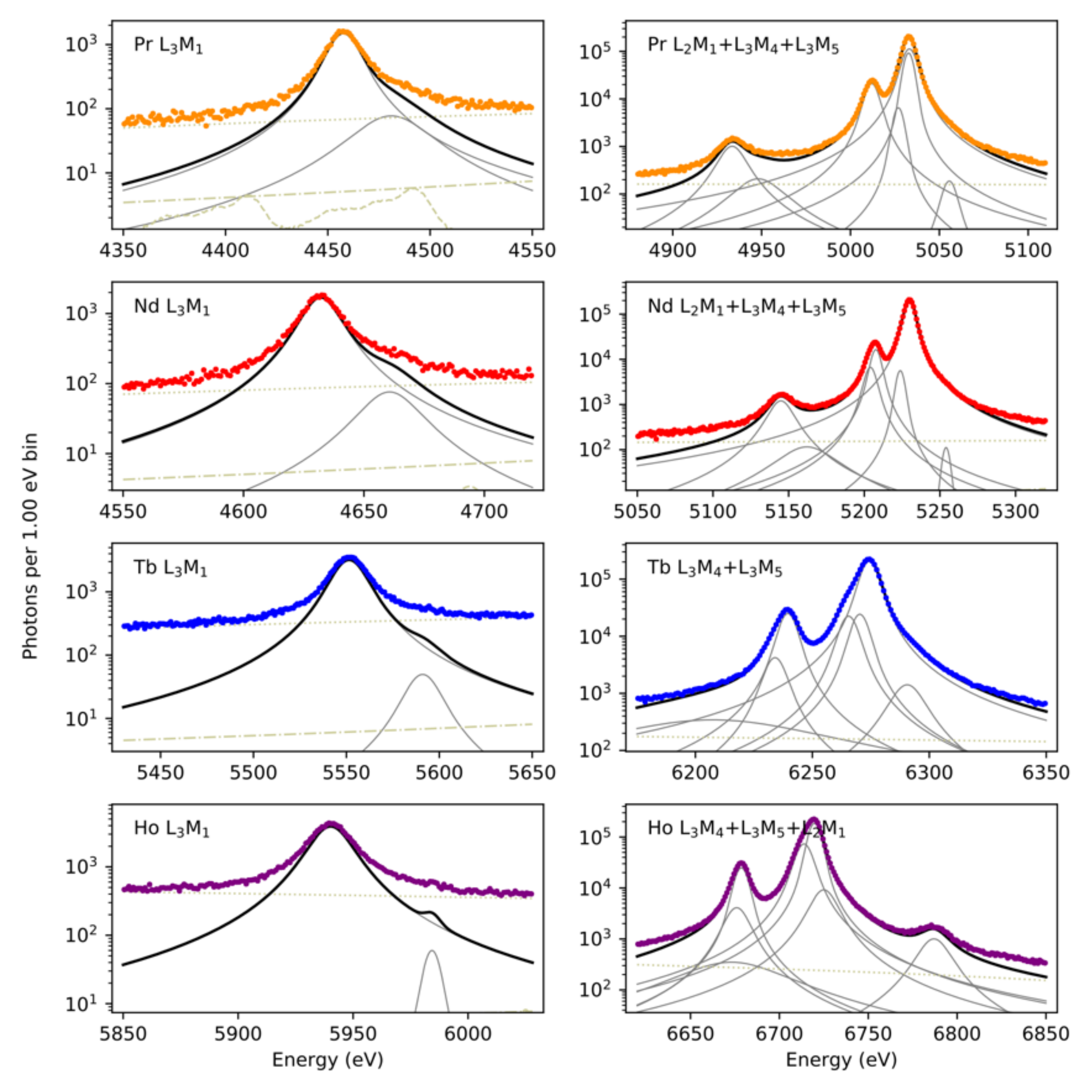

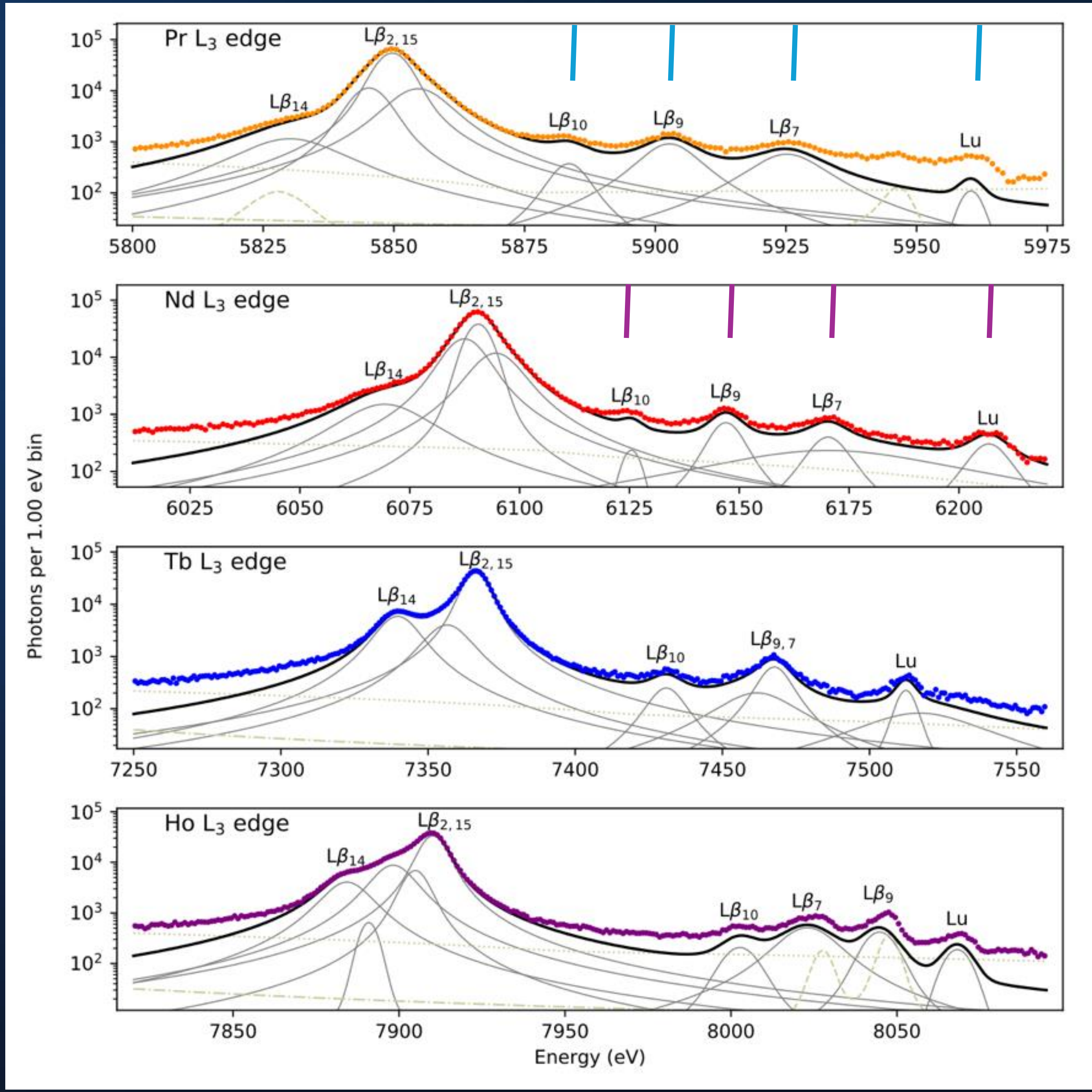

Summary of lanthanide campaign

- full line profiles for 97 lines from Nd, Tb, Ho, and Pr
  - 35 were absent from NIST's own reference data
  - the other 62 were only listed by peak energy

- median uncertainty on peak E reduced by at least 4x: 0.24 eV vs 0.94 eV

- see J. Fowler et al, *Metrologia* **58** (2021) 015016

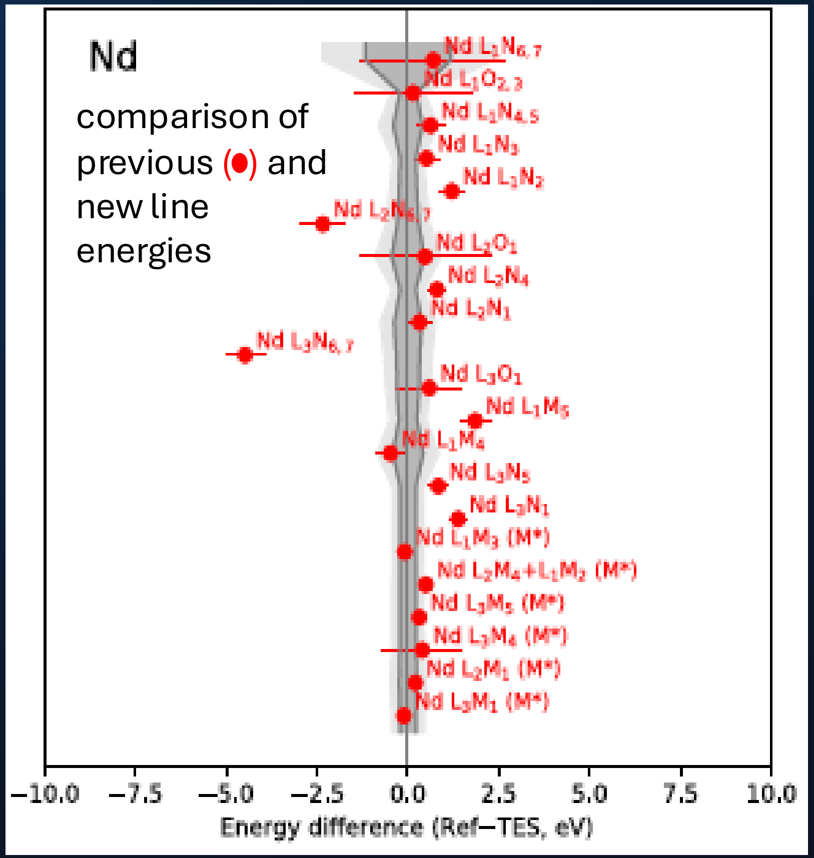

History of gamma-ray spectroscopy …

Hard x-ray and gamma-ray spectra from 5 different detectors

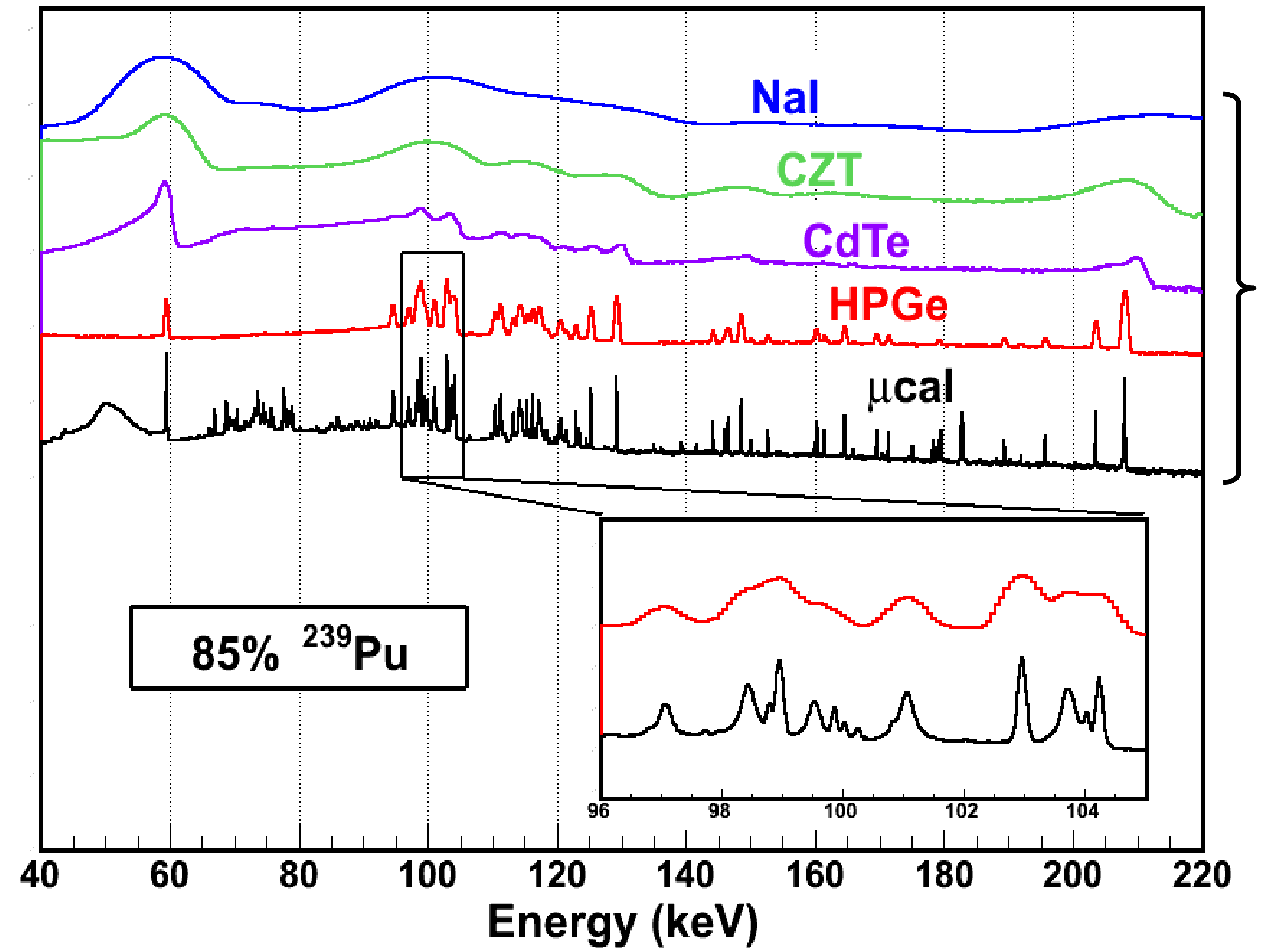

energy-dispersive gamma-ray detectors

ΔE_{HPGE} ~ 500 eV

ΔE_{TES} ~ 75 eV

Analysis of nuclear materials

TES γ-ray instruments. Attach bulk tin (Sn) absorber to thin-film TES to stop γ-rays.

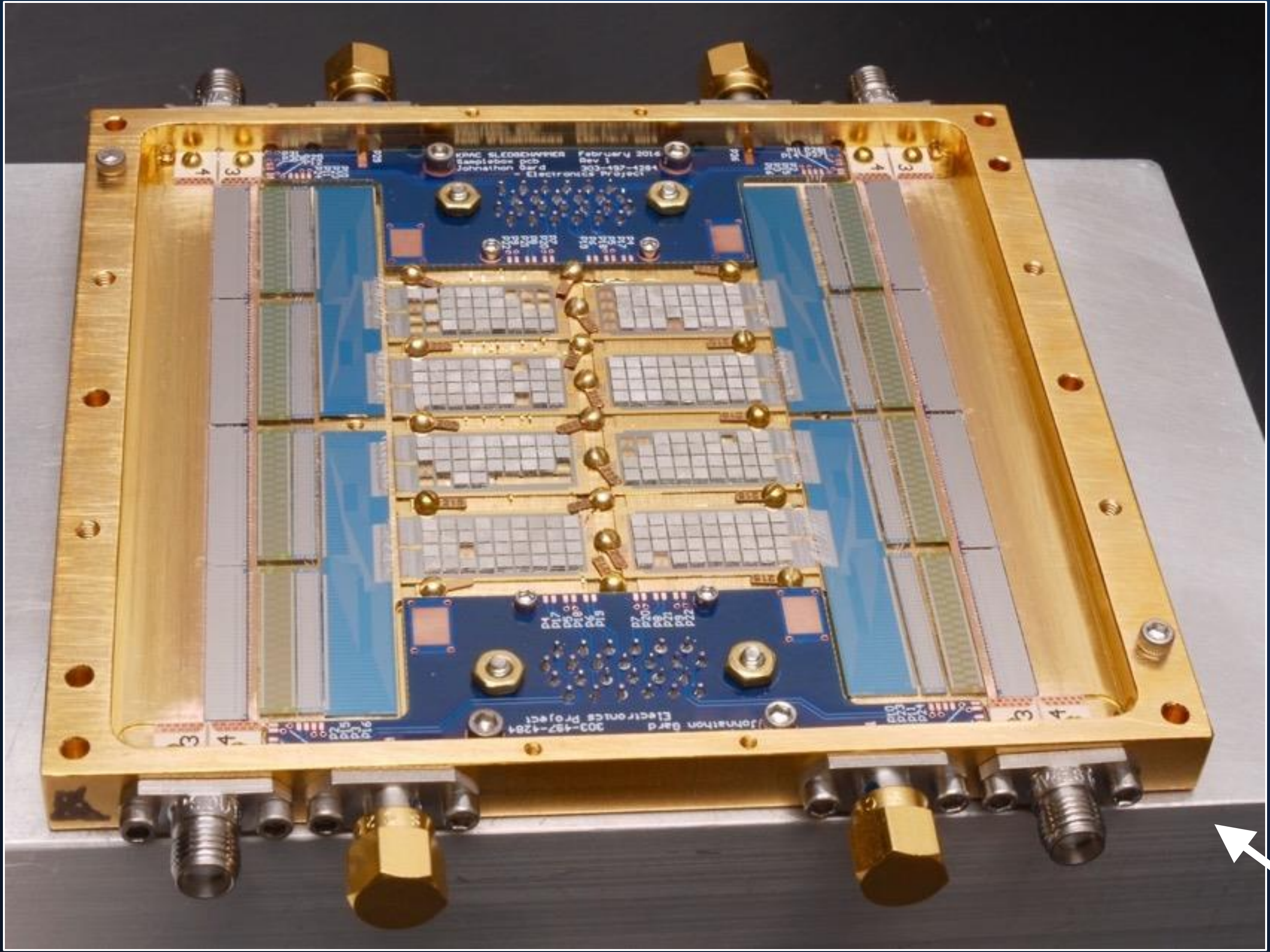

30 mm

20 mm

2D and 3D detector packages

Some active instruments

spectrometer in motion at LANL

spectrometer at INL

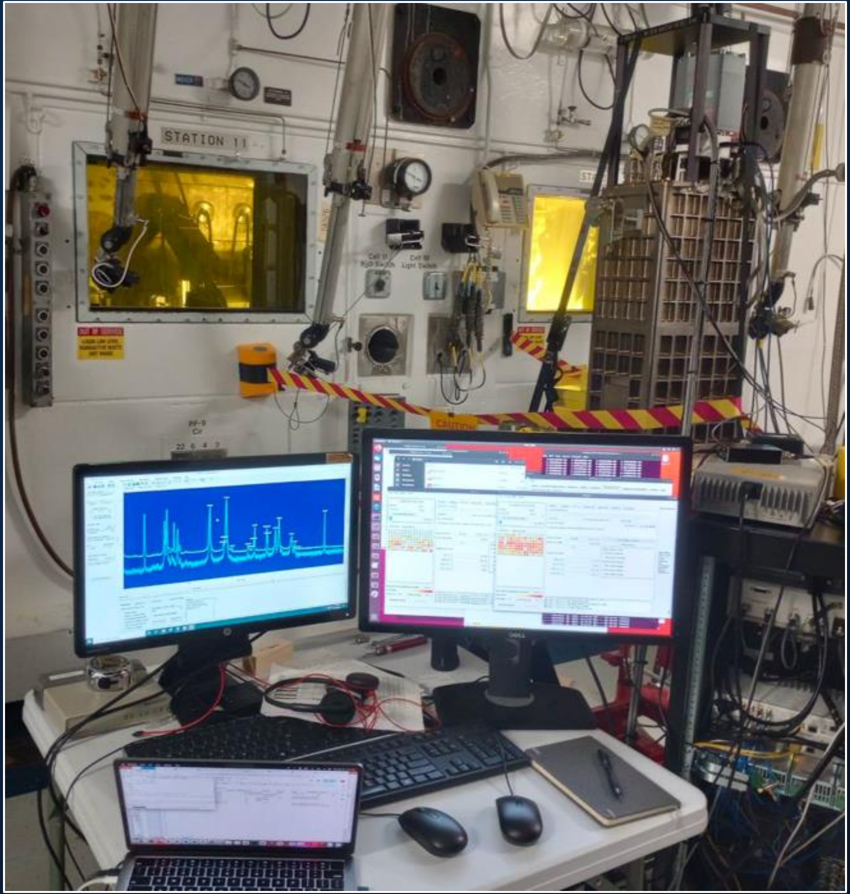

spectrometer visiting ORNL

also, spectrometer at PNNL and several others under construction

Lots of interesting measurements

- ‘extreme’ actinide assays
- assay of ^{242}Pu
- analysis of spent reactor fuel
- improved nuclear branching ratios
- discovery of new spectral lines
- improved actinide x-ray linewidths

Lots of interesting measurements

- ‘extreme’ actinide assays
- assay of ^{242}Pu
- analysis of spent reactor fuel
- improved nuclear branching ratios
- discovery of new spectral lines
- improved actinide x-ray linewidths

Pu-242 assay

- ^{242}Pu is present in Pu samples with extensive neutron exposure
- ^{242}Pu has a small number of weak γ-rays, and they are near other spectral features. It cannot presently be measured except in unusual, specially prepared samples.

“Plutonium-242 cannot be measured directly because of its low activity, low abundance, and weak gamma rays”

- From *Nondestructive Assay of Nuclear Materials for Safeguards and Security, 2nd ed.*

Pu-242 assay

- ^{242}Pu is present in Pu samples with extensive neutron exposure
- ^{242}Pu has a small number of weak γ-rays, and they are near other spectral features. It cannot presently be measured except in unusual, specially prepared samples.
- We have done the first non-destructive measurement of ^{242}Pu in unprepared, safeguards-relevant samples

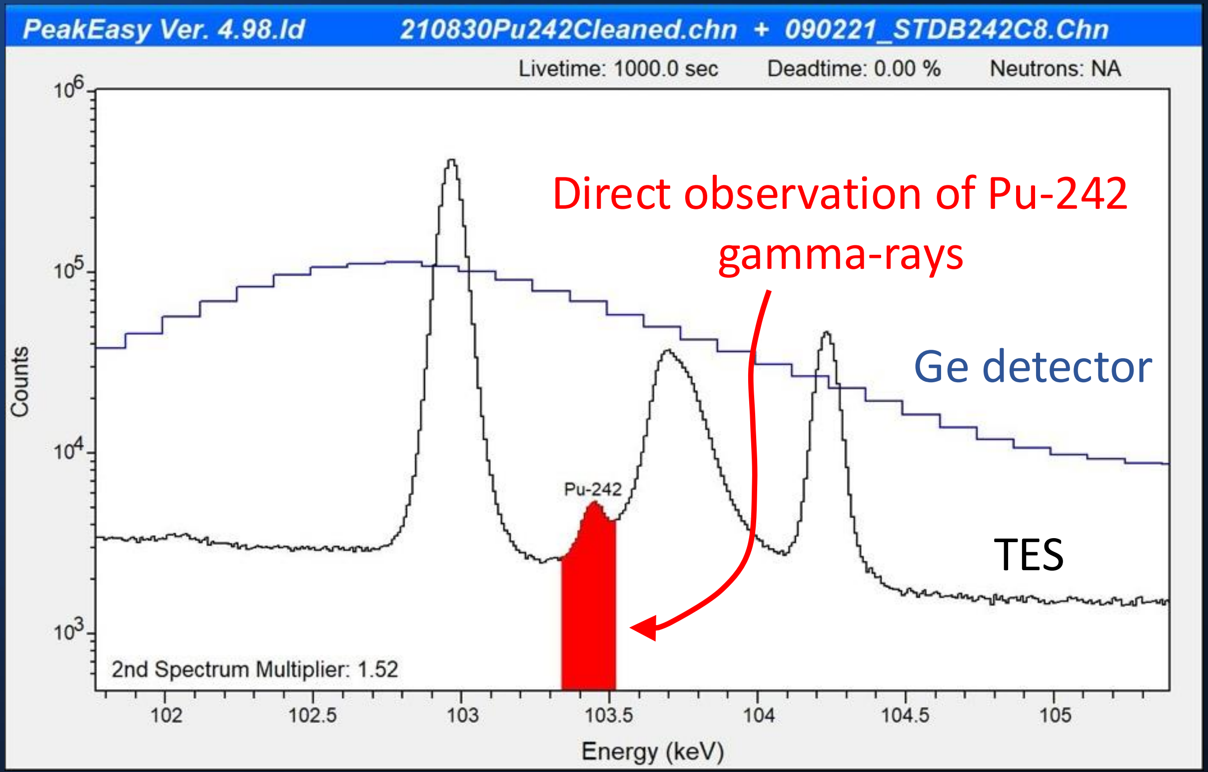

Data shown in this plot is unclassified and non-sensitive
See D. Mercer et al, http://arxiv.org/abs/2202.02933

Measuring Pu content in spent nuclear fuel

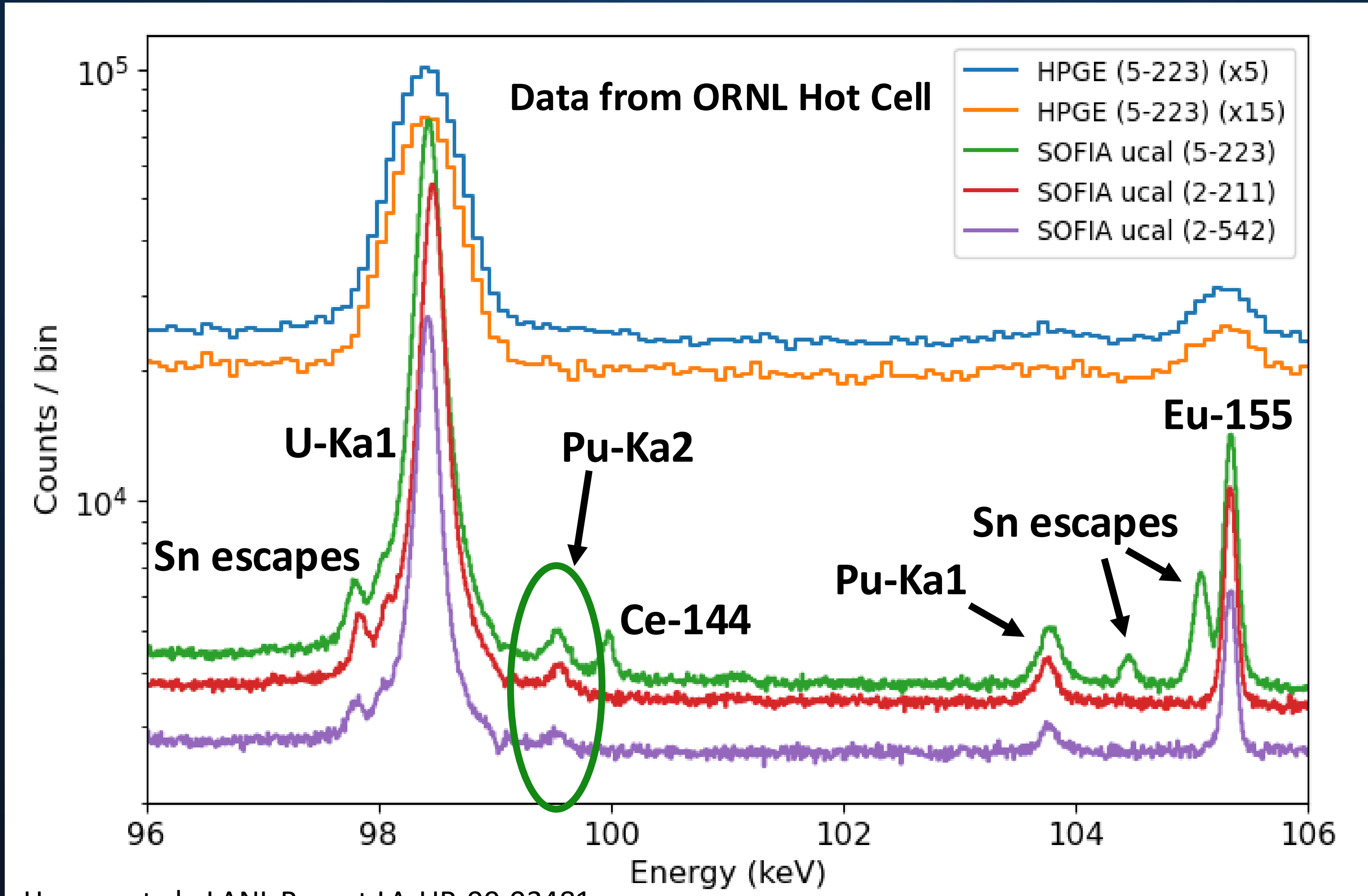

Hoover et al., LANL Report LA-UR-09-03481
Croce et al., LANL Report LA-UR-23-32266 (2023)

Microcal can see Pu x-ray fluorescence!

Naïve measurements of Pu/U ratio are within 5 – 13 % of calculated values

Synchrotron systems

- TES instruments at SSRL, NSLSII, BESSYII, APS
- TESs have also been used at SPRING8
- TES instruments at SSRL, NSLSII and BESSYII are for soft x-ray spectroscopy < 1 keV

Efficiency advantage of TES for soft x-rays

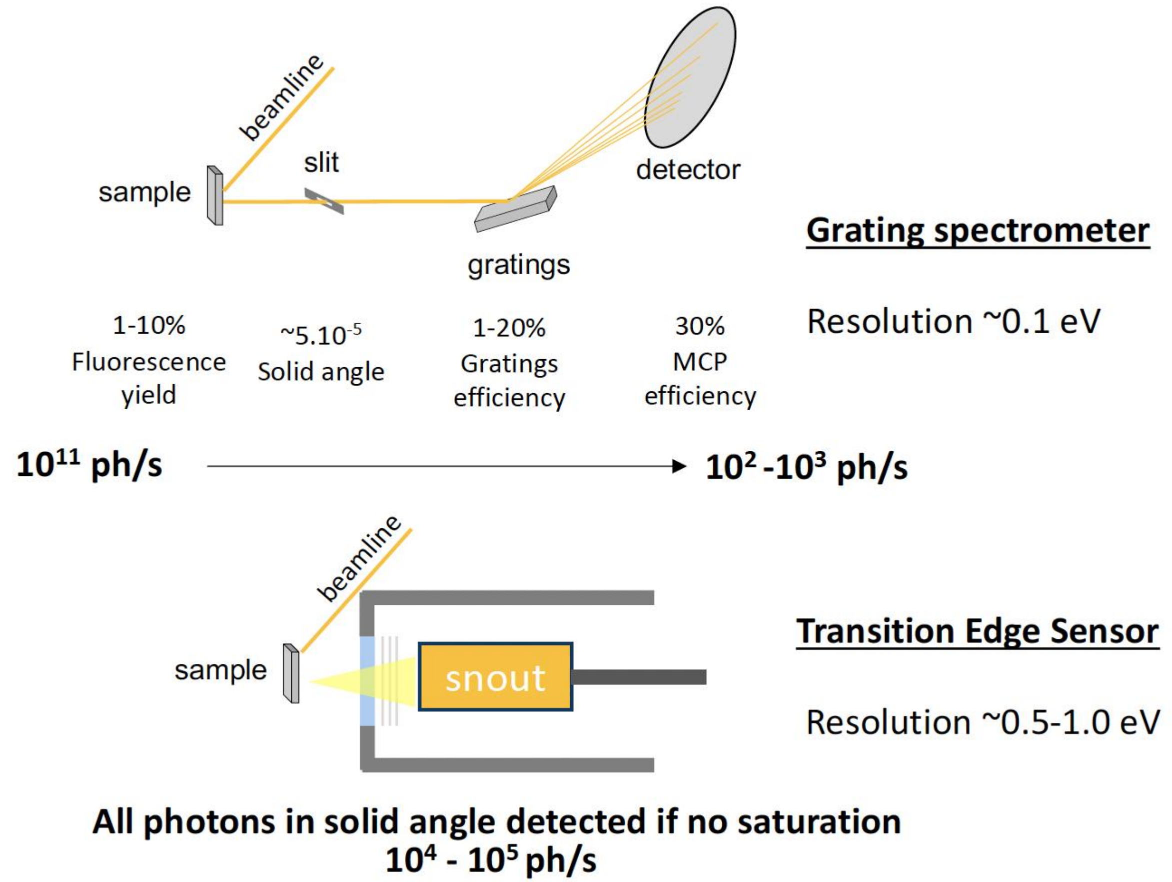

Figure from R. Decker, BESSYII

Today’s TES (~200 pixels) ~100x more sensitive than grating

Tomorrow’s TES (~2,000 pixels) ~1,000x more sensitive

Enabling properties of TESs for soft x-rays

- ΔE = 0.5 – 1.0 eV below 1 keV today, some potential to improve
- Much higher photon collection efficiency than gratings
- Instantaneously broadband response
- Resolving power independent of beam spot size -> can defocus beam to reduce radiation damage

TESs well matched to PFY-XAS, XES, and RIXS of dilute and fragile samples

Simultaneous acquisition of 3d2p and 3s2p features. Successful at extremely low concentrations

Titus et al, J. Chem. Phys. 147, 214201 (2017)

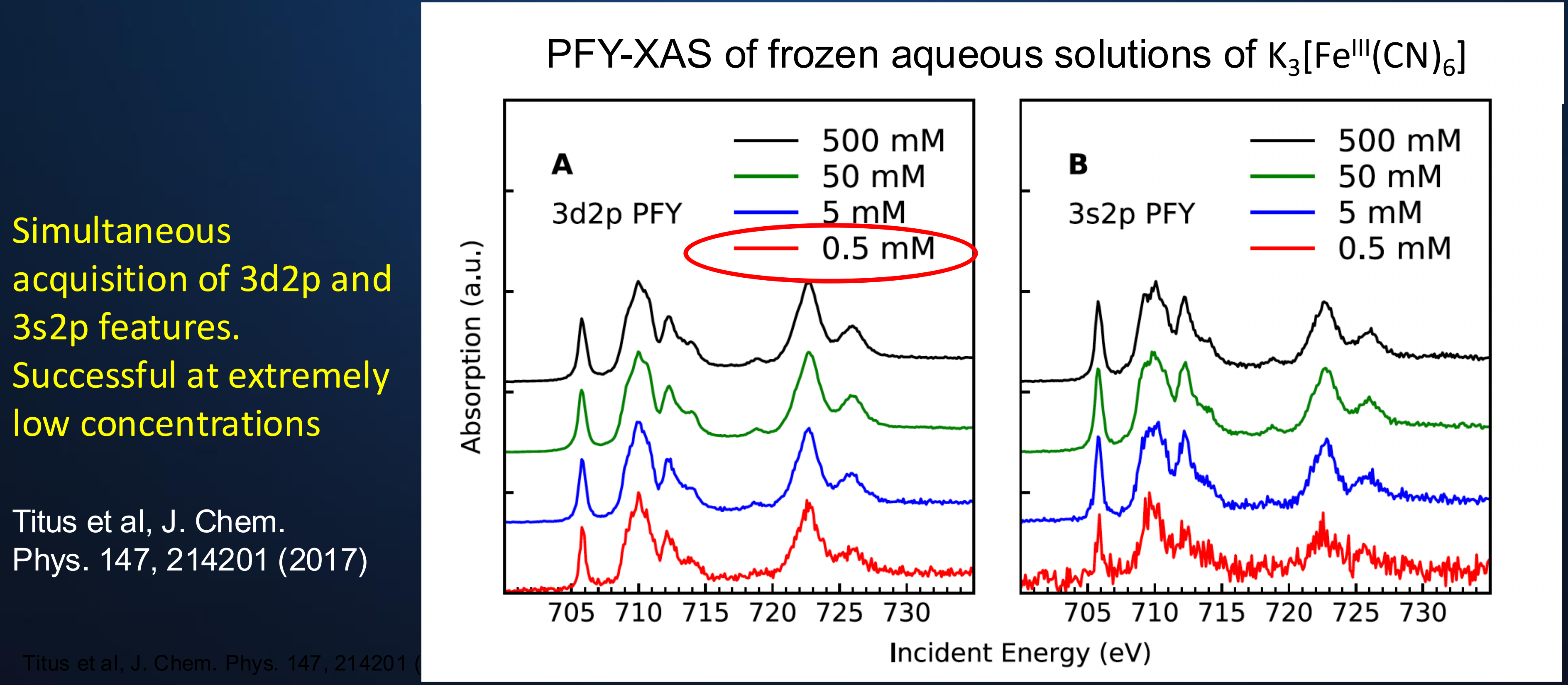

Structure of oxyhemoglobin

- Hemoglobin carries oxygen in blood
- Damage-sensitive proteins require highly efficient x-ray measurement methods (e.g. TES)
- Bonding physics of oxygenated hemoglobin debated since Linus Pauling (1936)
  - Fe^{II} or Fe^{III} ?
- Answer: about half-way between (57 ± 12% Fe^{III})

partial fluorescence yield (3s2p) Fe L-edge XAS of oxyhemoglobin

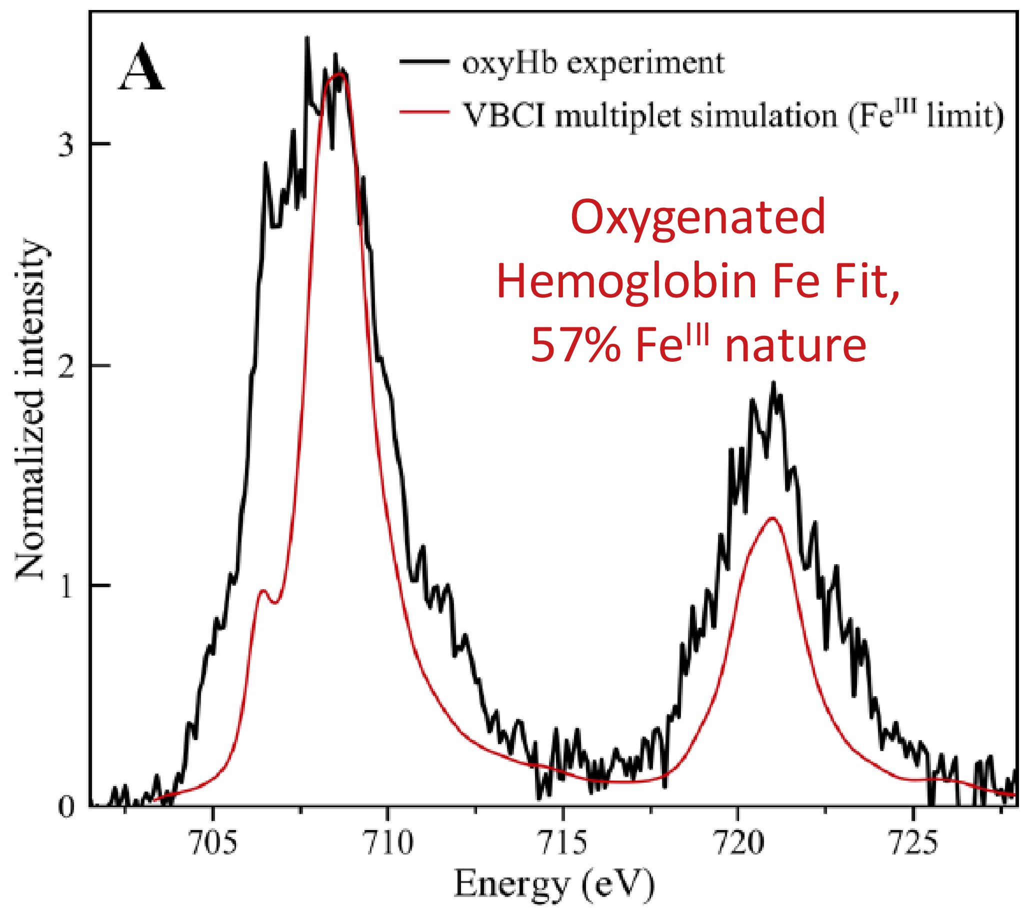

just published!

JACS
JOURNAL OF THE AMERICAN CHEMICAL SOCIETY
pubs.acs.org/JACS
Communication

Description of the Electronic Structure of Oxyhemoglobin Using Fe L-Edge X-ray Absorption Spectroscopy

Augustin Braun, Charles J. Titus, Leland B. Gee, Michael L. Baker, Max D. J. Waters, James J. Yan, Sang-Jun Lee, Dennis Nordlund, William B. Doriese, Galen C. O'Neil, Daniel R. Schmidt, Daniel S. Swetz, Joel N. Ullom, Kent D. Irwin, and Edward I. Solomon*

Improving absolute energy calibration

- At **intermediate energies (4-10 keV)**, transition metal K lines very well known and tied to SI – GOOD
- At **low energies (<3 keV)**, few good elemental calibrators because of broad and chemistry-dependent line shapes -> use multi-photon pulses from optical laser to build ladder of calibration features separated by few eV

X-ray spectrum overlayed with response to 400 nm laser pulses

Credit: Avirup Roy Wisconsin/ NIST

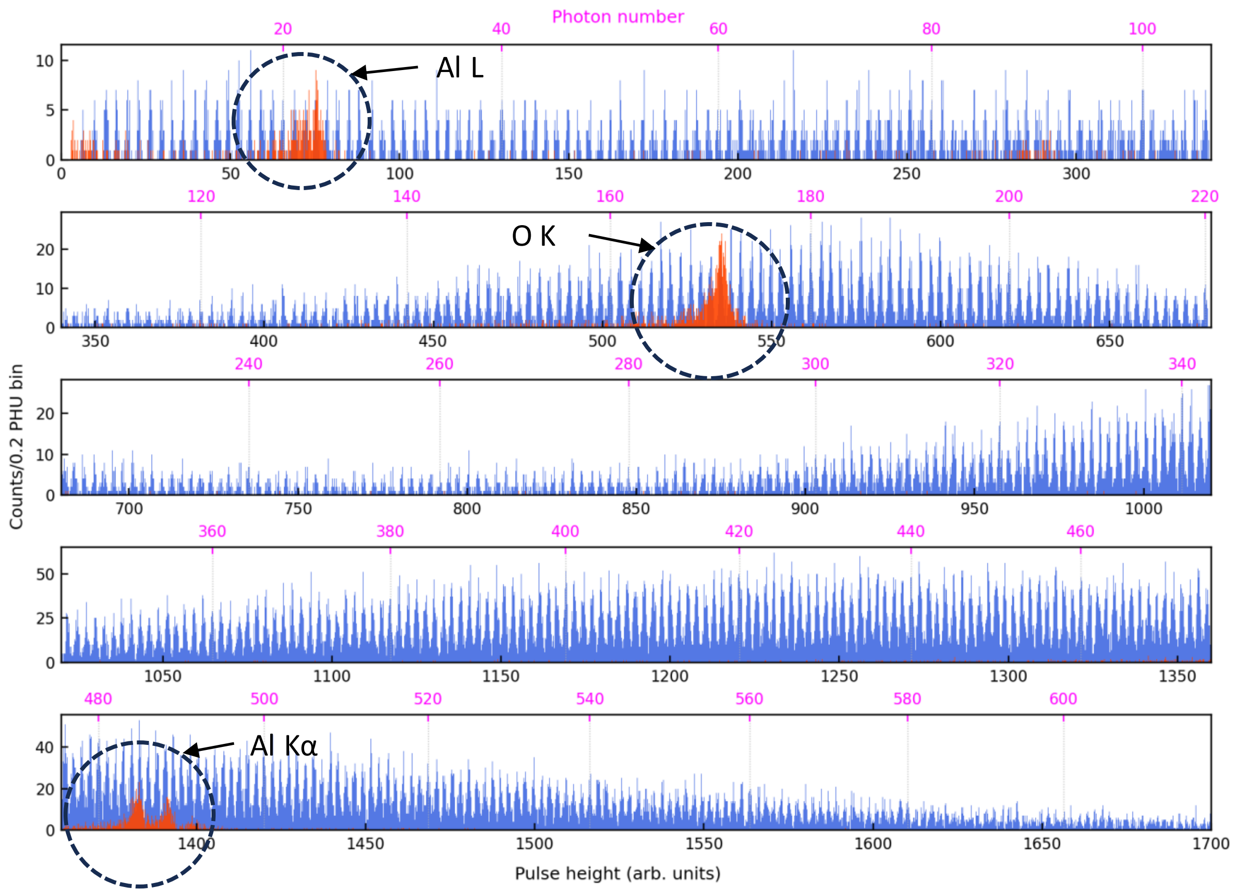

Illuminating all the TES pixels in an array at once introduces calibration errors because of cross talk -> **millikelvin scanning & focusing system to illuminate one pixel at a time**

cryogenic MEMs mirror

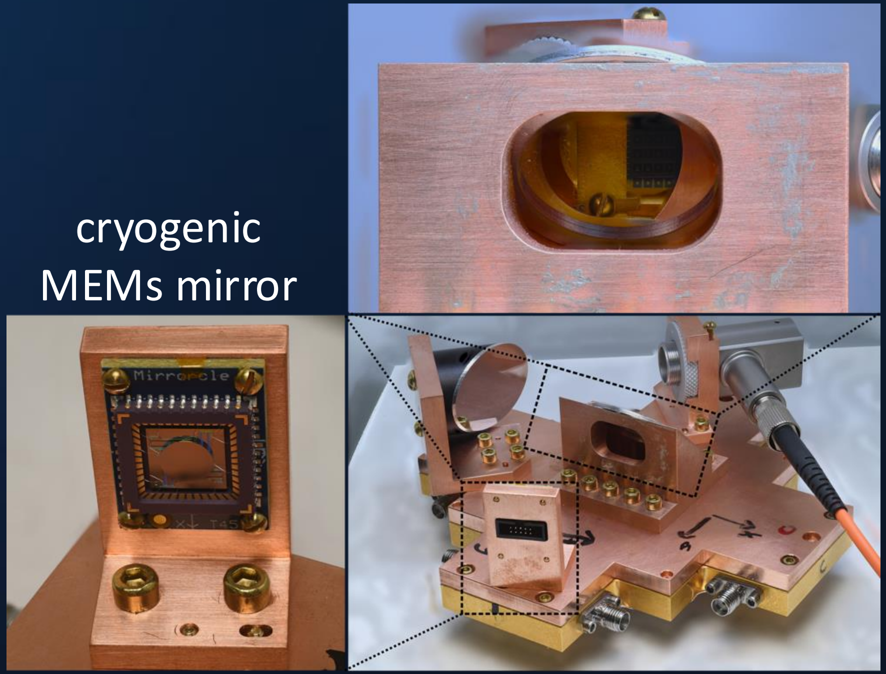

Progress towards larger, denser arrays

ready today

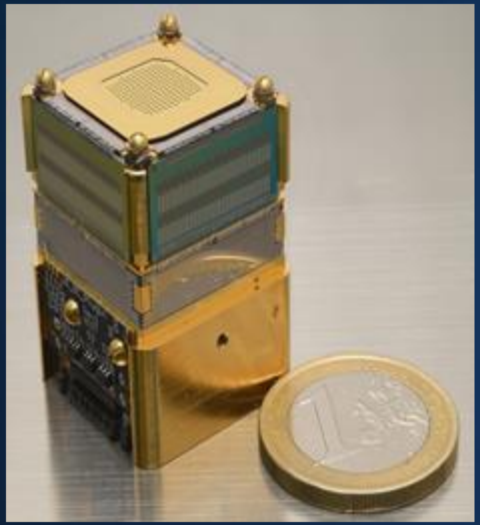

microsnout module: 250 10 keV TESs or 64 100 keV TESs

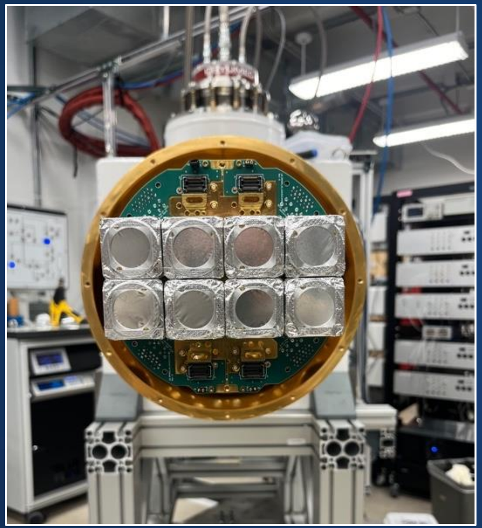

spectrometer with 2,000 live TESs and capacity for 3,000

- readout circuitry larger than sensor circuitry -> place on side of module
- sensors and readout on separate chips -> have to connect electrically
- connections made via wirebonds with ~100 um pitch
- size of module set by required length for wirebonds

Progress towards larger, denser arrays

ready today

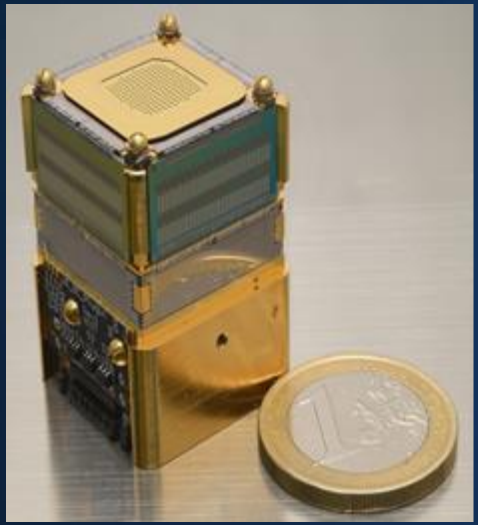

microsnout module: 250 10 keV TESs or 64 100 keV TESs

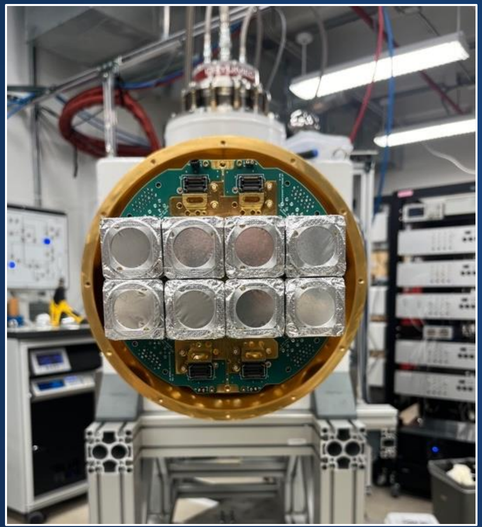

spectrometer with 2,000 live TESs and capacity for 3,000

- readout circuitry larger than sensor circuitry -> place on side of module
- sensors and readout on separate chips -> have to connect electrically
- connections made via wirebonds with ~100 um pitch
- size of module set by required length for wirebonds

under development

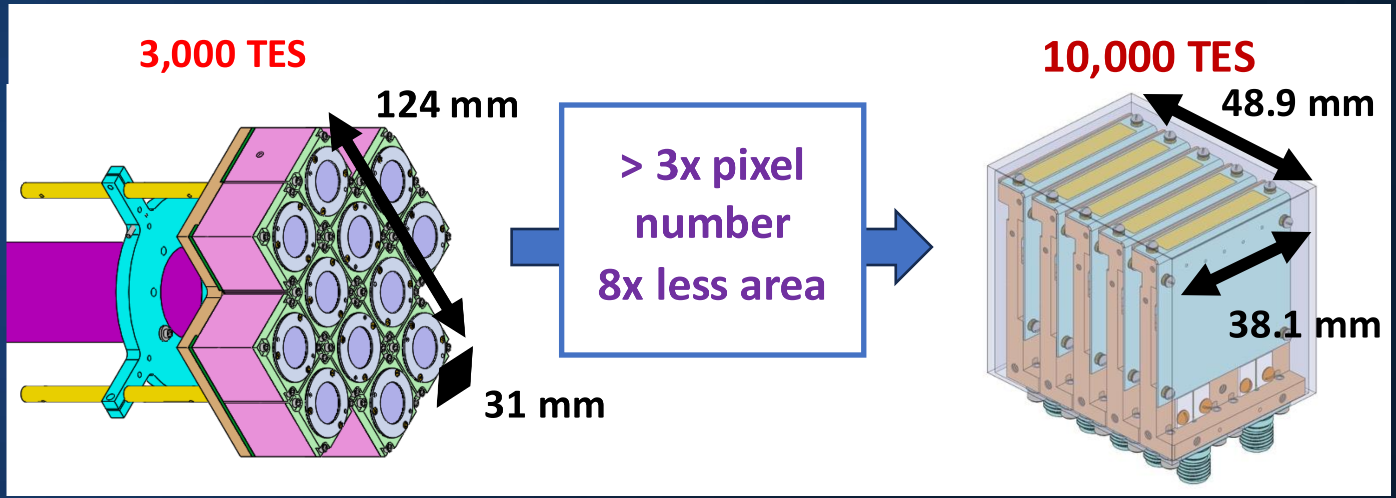

state-of-the-art: 12 μ-snouts

under development

- readout circuitry larger than sensor circuitry -> place on side of module
- sensors and readout on the same chip, **need to combine fabrication processes**
- connections made via lithographic features with < 10 um pitch
- **need to bend chip by 90 degrees**

Progress towards larger, denser arrays

ready today

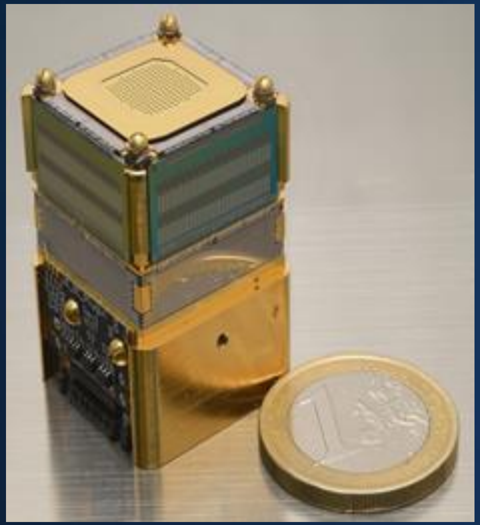

microsnout module: 250 10 keV TESs or 64 100 keV TESs

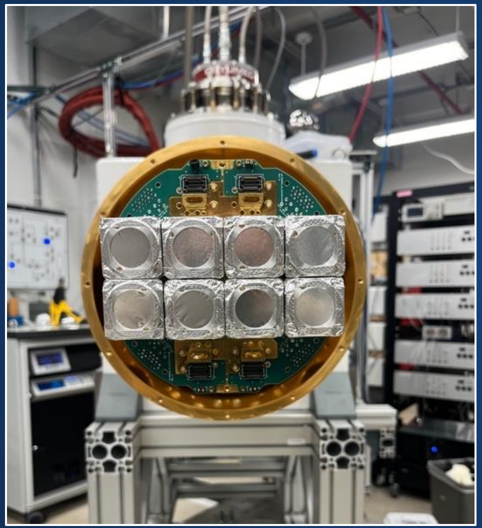

spectrometer with 2,000 live TESs and capacity for 3,000

- readout circuitry larger than sensor circuitry -> place on side of module
- sensors and readout on separate chips -> have to connect electrically
- connections made via wirebonds with ~100 um pitch
- size of module set by required length for wirebonds

under development

integrate microwave readout, L/R circuitry, and TES pixels on a single wafer

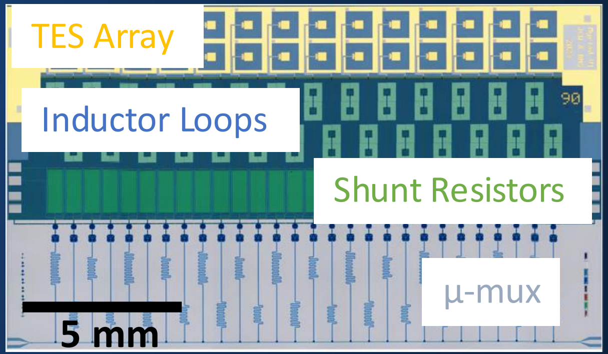

use thin, flexible Si to bend readout circuitry out-of-plane (provisional patent)

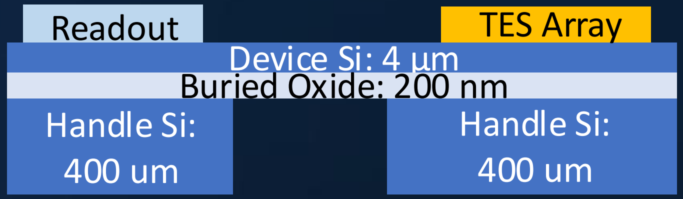

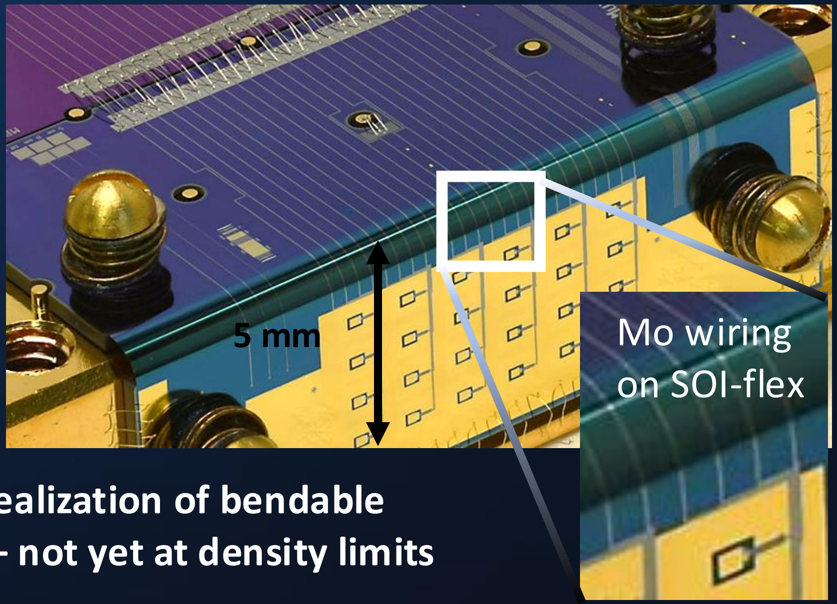

early realization of bendable circuitry – not yet at density limits

Summary

- microcalorimeter sensors cooled to sub-Kelvin temperatures can achieve noise performance near the thermodynamic limit, corresponding to eV-scale energy sensitivities
- arrays of microcalorimeter sensors provide a unique combination of resolving power (good) and collecting efficiency (also good). In particular, the collecting efficiency can far surpass that of crystals and gratings
- microcalorimeter arrays are well suited to photon-starved x-ray and gamma-ray measurements, especially measurements of dilute or radiation-sensitive samples
- closely related technology is used for rare-event searches and for studies of the cosmic microwave background, including an instrument with 10^5 TESs
- the technology is relatively new and significant performance improvements are likely

Thanks for your attention!